NIH-PA Author Manuscript

A Neurochemical Signature of Visual Recovery After Extrastriate Cortical Damage in the Adult Cat

Krystel R. Huxlin[*], **Jennifer M. Williams**, and **Tracy Price**
Department of Ophthalmology, University of Rochester, Rochester, New York 14642

Abstract

In adult cats, damage to the extrastriate visual cortex on the banks of the lateral suprasylvian (LS) sulcus causes severe deficits in motion perception that can recover as a result of intensive direction discrimination training. The fact that recovery is restricted to trained visual field locations suggests that the neural circuitry of early visual cortical areas, with their tighter retinotopy, may play an important role in attaining perceptual improvements after damage to higher level visual cortex. The present study tests this hypothesis by comparing the manner in which excitatory and inhibitory components of the supragranular circuitry in an early visual cortical area (area 18) are affected by LS lesions and postlesion training. First, the proportion of LS-projecting pyramidal cells as well as calbindin- and parvalbumin-positive interneurons expressing each of the four AMPA receptor subunits was estimated in layers II and III of area 18 in intact animals. The degree to which LS lesions and visual retraining altered these expression patterns was then assessed. Both LS-projecting pyramidal cells and inhibitory interneurons exhibited long-term, differential reductions in the expression of glutamate receptor (GluR)1, -2, -2/3, and -4 following LS lesions. Intensive visual training post lesion restored normal AMPAR subunit expression in all three cell-types examined. Furthermore, for LS-projecting and calbindin-positive neurons, this restoration occurred only in portions of the ipsi-lesional area 18 representing trained visual field locations. This supports our hypothesis that stimulation of early visual cortical areas—in this case, area 18—by training is an important factor in restoring visual perception after permanent damage to LS cortex.

Indexing terms

GluR1; GluR2; GluR3; GluR4; NR1; calbindin; parvalbumin; pyramidal cell

---

The adult brain exhibits remarkable plasticity throughout life (see reviews by Gilbert et al., 1996; Kaas, 1995). Well-documented cases of training-induced recovery following damage to adult motor cortex (see reviews by Hallett, 2001; Cauraugh and Summers, 2005), adult somatosensory cortex (Xerri, 1998; Xerri et al., 2004), and adult visual cortex (Newsome and Pare, 1988; Rudolph and Pasternak, 1996, 1999; Huxlin and Pasternak, 2004) suggest that some of this plasticity can be tapped for the purpose of recovering function after permanent brain damage. In the visual system, most studies reporting training-induced recovery of function were conducted following damage to extrastriate visual cortex—lesions of the lateral suprasylvian (LS) visual cortex in cats, e.g. (Rudolph and Pasternak, 1996; Huxlin and

*Correspondence to: Krystel R. Huxlin, Ph.D., Department of Ophthalmology, Box 314, University of Rochester Medical Center, 601 Elmwood Ave, Rochester, NY 14642. huxlin@cvs.rochester.edu.

Pasternak, 2004) or lesions in areas MT/MST of monkeys (Newsome and Pare, 1988; Rudolph and Pasternak, 1999).

The feline LS cortex is a complex of extrastriate visual areas (Palmer et al., 1978; Sherk, 1986b; Grant and Shipp, 1991; Sherk and Mulligan, 1993) that exhibit functional similarity with areas MT/MST of primates (Payne, 1993), playing an important role in the processing of complex visual motion information (Rauschecker, 1988; Rudolph and Pasternak, 1996; Akase et al., 1998). LS cortex is relatively high level in the hierarchy of the cat visual system (Scannell et al., 1995). It receives a predominant feed-forward input from early visual cortical areas 17, 18, and 19 (Fig. 1) (Symonds and Rosenquist, 1984; Sherk, 1986a,b; Shipp and Grant, 1991). However, the relative contribution of these early visual areas to receptive field properties in LS cortex is not equal. Indeed, electrophysiological response properties of many LS neurons reflect their input from area 18 more than that from any other visual cortical area (Dreher et al., 1996; Lee et al., 1998). Previous lesion studies also revealed differences in the strength of the interactions between LS cortex and its input from areas 17, 18, and 19, with the strongest interactions involving area 18 (Huxlin and Pasternak, 2001).

Unilateral lesions of LS cortex in adult cats cause contralateral deficits in complex motion perception that are capable of recovery (Rudolph and Pasternak, 1996; Huxlin and Pasternak, 2004). However, recovery depends not on the passage of time or normal visual experience post lesion, but on animals being intensively retrained to discriminate the direction of motion of complex stimuli within impaired portions of their visual field (Huxlin and Pasternak, 2004). Furthermore, training-induced recovery after LS lesions is always restricted to retrained visual field locations (Huxlin and Pasternak, 2004). The tighter retinotopic organization of early visual cortical areas (relative to higher level visual cortical areas: Palmer et al., 1978; Tusa et al., 1981; Sherk and Mulligan, 1993) suggests that recovery might be mediated by early levels of the visual cortical system. Area 18, a relatively low-level area in the cat visual cortical hierarchy, might be an ideal candidate to mediate training-induced recovery after LS lesions because of its strong interconnections with LS cortex.

Previously, we showed that the neuronal expression of calcium-binding proteins (Huxlin and Pasternak, 2001) and AMPA receptor subunits (Price and Huxlin, 2001) in superficial layers of area 18 was downregulated after LS lesions. The present study tests the prediction that if area 18 were to play a critical role in mediating training-induced recovery of motion perception after a lesion of LS cortex, neurochemical changes induced by the LS lesion should be reversed in a retinotopic manner, i.e., primarily in area 18 neurons that respond to regions of the visual field exposed to visual stimuli used during retraining.

In the adult neocortex, AMPA receptors, one of the major ionotropic glutamate receptors, mediate most fast excitatory synaptic transmission (Tsumoto et al., 1987; Fox et al., 1989; Tsumoto, 1990; Carmignoto and Vicini, 1992; Fox et al., 1992; Fox and Daw, 1993). They are comprised of four subunits—GluR1, GluR2, GluR3, and GluR4—that are differentially expressed in different neurons (Vickers et al., 1993; Geiger et al., 1995; Vissavaijhala et al., 1996; Angulo et al., 1997; Kondo et al., 1997; Munoz et al., 1999; Van Damme et al., 2003). Although many glutamate receptors (such as AMPA, N-methyl-D-aspartate [NMDA], kainate) play a role in activity-dependent neuronal plasticity (Collingridge and Singer, 1990; Malenka and Nicoll, 1993), the sensitivity of AMPA receptor to changes in connectivity and function within the cat visual system has been well demonstrated (Gordon et al., 1996; Price and Huxlin, 2001; Van Damme et al., 2003).

Subtle changes in the subunit composition of AMPA receptors, just like changes in NMDA receptor subunit composition, can both cause and result from significant changes in neuronal function (Liao et al., 1995, 1999; Rumpel et al., 1998; Petralia et al., 1999; Liu and Cull-Candy,

2000; Malinow and Malenka, 2002; Bredt and Nicoll, 2003), as demonstrated during experience-dependent synaptic refinement in developmental critical periods (Rumpel et al., 1998; Bear and Rittenhouse, 1999; Lu and Constantine-Paton, 2004) and during behavioral plasticity in adulthood (Carroll and Zukin, 2002; Ehrlich and Malinow, 2004; Schmitt et al., 2004). Thus, if the perceptual relearning or recovery induced by intensive visual retraining after LS lesions, like most instances of cortical plasticity, is mediated by changes in excitatory neuronal function within area 18, we predict that this should be associated with significant, cell-type-specific, and retinotopically specific changes in the expression of AMPA receptor subunits within area 18.

MATERIALS AND METHODS

Subjects

Nine adult female and male cats were used in experiments conducted according to the NIH Guidelines for the Care and Use of Laboratory Animals (NIH Publication no. 86-23, revised 1987) and following the recommendations of the University of Rochester's Committee on Animal Resources.

Cats 1, 2, and 3 were pretrained to perform left-right direction discrimination at different visual field locations, with controlled fixation. They then received unilateral LS lesions and underwent retraining of complex motion perception at a single location in their impaired hemifield, as described in our previous publication (Cats 1 and 2 = Cats A and C in Huxlin and Pasternak, 2004; see Behavioral Procedures section below). Cats 1, 2, and 3 were designed to act as their own internal controls for the effects of LS lesions, prelesion training, motivational factors, and exposure to normal visual experience on cortical neurochemistry. Two classes of external controls were also used: Cats 4, 5, and 6 received either unilateral (Cat 6) or bilateral (Cats 4 and 5) LS lesions but were *not* behaviorally trained or tested before or after lesioning. This allowed us to separate the impact of LS lesions from that of visual training on glutamate receptor subunit expression in area 18.

Finally, Cats 7, 8, and 9 received no lesions or behavioral training. Their brains were processed for immunohistochemistry to establish a baseline of normal glutamate receptor subunit expression in completely intact animals that were not behaviorally manipulated. This was critical to establishing that glutamate subunit expression in area 18 of the intact hemispheres of Cats 1, 2, and 3 was not "normal" and instead, exhibited "lesion-like" characteristics.

Behavioral protocols

Prelesion training—Before undergoing unilateral lesions of LS cortex, Cats 1, 2, and 3 were pretrained to perform a two-alternative, forced-choice, direction discrimination task with controlled fixation both centrally and up to about 15° eccentricity in each of their four visual field quadrants (Fig. 2A–C). Eye position was monitored with magnetic search coils (Remmel, 1984) and subconjunctival eye coils implanted unilaterally in each animal. During training or testing, each cat was placed inside a magnetic field generated by a set of 50-cm field coils. Its head was immobilized by using an implanted head-holder, and electrical signal from its eye coil was detected and calibrated by using an eye coil phase detector (Riverbend Electronics, Rushford, MN). The animals were first trained to position their gaze within an electronically defined, square window 1–1.5° in diameter, centered on a bright fixation spot presented on a 19-inch computer monitor in front of them. They were then trained to discriminate between left- and rightward global motion of a visual stimulus in a two-alternative forced-choice paradigm (Fig. 2D).

Steady fixation of the fixation spot for 800–1,000 ms resulted in a tone signaling the onset of the trial and presentation of a 500-ms stimulus during which the cats were required to maintain fixation. After the stimulus and the fixation spot were extinguished, two "response targets", separated by 10° of visual angle, appeared. Cats were required to saccade to the rightmost response target for rightward moving stimulus, and to the leftmost response target for leftward drifting stimuli. The sequence of presentation of rightward and leftward drifting stimuli was randomized. Each correct response was rewarded with pureed beef. Incorrect responses resulted in a 3-second tone and no food reward. A break in fixation during stimulus presentation produced a 1-second tone and the termination of the trial, which was not included in the final analysis. Daily testing sessions consisted of 200–300 trials each.

Before their lesion, Cats 1, 2, and 3 were trained to discriminate the direction of motion of random dots stimuli consisting of bright dots (luminance ~3.5 log units above human detection threshold), 0.03° in diameter, randomly distributed within a circular aperture 4 or 5° in diameter on a dark background (mean luminance = 0.1 cd/m^2). Individual dots had a lifetime of 250 ms and a density of 2.6 dots/deg^2. They moved at a speed of 20 deg/sec ($\Delta t = 13$ ms, $\Delta x = 0.26°$) and were repeatedly displaced in a direction chosen randomly from a uniform distribution of directions, with a new set generated on each frame. A staircase procedure was used to measure a direction range threshold at each visual field location trained. To do so, the range of dot directions in the stimulus was varied from the easiest (direction range = 0°) to the most difficult level (direction range = 355°) in 40° steps. Three consecutive correct responses at one level resulted in presentation of a less discriminable stimulus. An incorrect response decreased stimulus difficulty by one level.

Thresholds from each session were estimated by fitting a Weibull function (Weibull, 1951) to the data and computing the direction range level that allowed the cats to attain 75% correct. Prelesion training continued until thresholds stabilized (coefficient of variation ≤ 10% of the mean over at least five data points) at multiple locations in each visual field quadrant (Fig. 2A–C), chosen so as to stimulate the left and right hemifield of each cat fairly equivalently. Once basic training was completed, Cats 2 and 3 received unilateral injections of DiI into LS cortex. Two weeks later, all three cats received ibotenic acid lesions of LS cortex unilaterally.

Postlesion assessment of visual deficit—Cats 1–3 started visual testing 1–2 weeks after their LS lesion. Direction range thresholds were first measured in the hemifields ipsilateral to the lesions to verify that the animals had not forgotten how to perform the left-right, direction discrimination task and that they were sufficiently motivated to attain at least preoperative levels of performance. Once this was confirmed, thresholds were then measured in the hemifields contralateral to the damaged hemisphere to assess the magnitude of the visual deficit induced by the lesion.

Postlesion visual retraining—A single visual field location was selected as the site of visual retraining in each animal. Prerequisites for selecting this location were that it had to be deep within the blind region of the visual field and that at this site, the cats were completely unable to discriminate the direction of coherently moving random dot stimuli (direction range threshold = 0°), a characteristic of LS lesions (Huxlin and Pasternak, 2004; Rudolph and Pasternak, 1996). The chosen locations, represented by solid black circles (a, b, and c) in Figure 3A, were in the left lower visual quadrant in Cat 1, the left upper quadrant in Cat 2, and the right lower quadrant in Cat 3. Retraining consisted of daily sessions in which Cats 1–3 performed a two-alternative, forced-choice, left-right direction discrimination task at the chosen location. All three cats exhibited a gradual recovery of direction range thresholds over 15–40 retraining sessions (Huxlin and Pasternak, 2004) so that their final thresholds were not significantly different from normal, as measured at equivalent locations in their intact hemifields (Fig. 3B).

Following recovery at the retrained locations, thresholds were measured at several non-overlapping sites, at increasing distances away from these locations (Fig. 4A–C) in order to verify that training-induced improvements of direction range thresholds were limited to retrained portions of the visual field, as previously reported (Huxlin and Pasternak, 2004).

Injection of DiI into LS cortex

All cats except for Cat 1 received injections of DiI into LS cortex in order to label LS-projecting neurons retrogradely in area 18. Cats were sedated with ketamine (15 mg/kg) and deeply anesthetized with 2% isoflurane before being placed in a stereotaxic apparatus. A craniotomy was made from 5 mm posterior to 15 mm anterior to the interaural line and from 8 to 17 mm lateral to the midline. The dura was cut, and the cortex on the banks of the lateral suprasylvian sulcus was exposed. A 5% solution of the carbocyanine, lipophilic tracer DiI (D-282, Molecular Probes, Eugene, OR) diluted in dimethyl sulfoxide (DMSO) was injected into LS cortex. Once DiI is transported to the cell body, it survives there for months to years without degradation, toxicity, or significant transfer to surrounding cells (Honig and Hume, 1986, 1989; Kuffler, 1990). About 20 injections, each of 100 nl of 5% DiI in DMSO, were made into the banks of the lateral syprasylvian sulcus in each animal by using a 5-µl Hamilton syringe fitted with a 32-gauge needle. Injection sites were spaced at 1.5-mm intervals, starting 1–3 mm posterior to and extending to about 10–12 mm anterior to the interaural line. For Cats 2–6, ibotenic acid lesions of LS cortex were made 2 weeks after the DiI injections. Care was taken to ensure that toxin injections extended further posteriorly and anteriorly than DiI injections, which was easily verified by visual inspection of the pink-stained areas of LS cortex resulting from DiI injections.

Ibotenic acid lesions of LS cortex

Cats were sedated with ketamine (15 mg/kg) and deeply anesthetized with 2% isoflurane before being placed in a stereotaxic apparatus. The original craniotomy was reopened to expose the cortex on the banks of the lateral suprasylvian sulcus. Thirty to forty injections, each of 0.5–1 µl of sterile ibotenic acid (Sigma [St. Louis, MO], 10 mg/ml in 0.1 M phosphate buffered saline [PBS], pH 7.4), were made into both banks along the entire length of the LS sulcus in order to destroy its gray matter permanently. All injections were made by using a 10-or 25-µl Hamilton syringe fitted with a 32-gauge, beveled needle. Injection sites were spaced at intervals of 1.7 mm across the cortical surface, starting 3 mm posterior to the interaural line and ending about 14 mm anterior to the interaural line. The separation of the injections and the amount and concentration of ibotenic acid injected were previously shown to produce contiguous lesions (Huxlin and Pasternak, 2001, 2004).

Histology and lesion reconstructions

At the end of the experiment, all cats were sedated with an intramuscular injection of 20 mg/kg ketamine before undergoing euthanasia with an overdose of sodium pentobarbital (100 mg/kg, intraperitoneally). They were then perfused with 3% paraformaldehyde and 0.1% glutaraldehyde in 0.1 M phosphate buffer (PB), pH 7.4. Once the brains were adequately cryoprotected, serial frozen sections were cut in the coronal plane, at a thickness of 40 µm. Alternate sections were reacted for cytochrome oxidase (CO), a marker of neuronal activity that can be used to delineate precisely brain regions where neurons have been killed, and for Nissl substance with cresyl violet. For the CO reaction, free-floating brain sections were incubated at 37°C for 3–4 hours in a solution of 0.06% diaminobenzidine tetrahydrochloride (Sigma), 0.03% cytochrome C (Type III, Sigma), and 4.4% sucrose in 0.1 MPB. Once the sections reached the appropriate dark brown coloring, they were rinsed and mounted onto subbed slides for analysis.

The cortical areas damaged by the ibotenic acid injections were verified by using Nissl- and CO-stained sections. In sections stained with cresyl violet, the damaged portions of cortex were characterized by the absence of identifiable neurons, the presence of gliosis, and vacuoles. In sections stained for CO, damaged cortex was identified by the lack of brown staining in the gray matter. The damaged cortical areas were identified by matching stained coronal brain sections with published electrophysiological maps (Tusa et al., 1981). The Nissl stain was also used to identify cortical layers and help distinguish borders between some cortical areas.

Double-labeling immunohistochemistry

Free-floating coronal brain sections were reacted for 12–24 hours with a cocktail of anti-calbindin antibody, anti-parvalbumin antibody, or DiI (LS-projecting cells were retrogradely labeled with DiI), along with one of several different glutamate receptor antibodies. Primary antibodies used were as follows:

1. Anti-calbindin (Sigma, catalog #C-8666, lot #074H4816, mouse monoclonal IgG1 from ascites fluid, clone CL-300, raised against calbindin-D 28kD from chicken gut).

2. Anti-parvalbumin (Sigma, catalog #P-3171, lot #055H4819, mouse monoclonal IgG1 from ascites fluid, clone PA-235, raised against parvalbumin purified from carp muscle).

3. Anti-NMDAR1 (Chemicon [Temecula, Ca], catalog #AB1516, lot #24795284, affinity-purified polyclonal antibody made in rabbit with synthetic peptide LQNQKDTVLPRRAIEREEGQLQLCSRHRES corresponding to the C-terminus of rat NMDA receptor subunit 1).

4. Anti-GluR1 (Chemicon, catalog #AB1504, lot #22010675, affinity-purified polyclonal antibody made in rabbit against C-terminus peptide of rat GluR1 [SHSSGMPLGATGL] conjugated to bovine serum albumin [BSA] with gluteraldehyde).

5. Anti-GluR2 (Chemicon, catalog #AB1768, lot #23100618, affinity-purified polyclonal antibody made in rabbit against a synthetic peptide from amino acids 827–842 of the rat GluR2, conjugated to BSA through a cysteine added to the C-terminus of the peptide).

6. Anti-GluR2/3 (Upstate Biotechnology [Lake Placid, NY], catalog #06-307, lot #24828, affinity-purified polyclonal antibody made in rabbit against a 21-residue synthetic peptide [KQNFATYKEGYNVYGIESVKI] corresponding to the C-terminal of rat GluR2 with a lysine added at the N-terminus).

7. Anti-GluR4 (Chemicon, catalog #AB1508, lot #21081551, affinity-purified polyclonal antibody made in rabbit against the C-terminus peptide of rat GluR4 [RQSSGLAVIASDLP] conjugated to BSA with gluteraldehyde).

The mouse monoclonal anti-calbindin antibody used reacts specifically with the Ca-binding spot of calbindin-D (MW = 28,000, pI = 4.8) from human, monkey, rabbit, rat, mouse, chicken, hamster, sheep, guinea pig, and fish in two-dimensional immunoblots (manufacturer's technical information). The mouse monoclonal anti-parvalbumin antibody used reacts specifically with the Ca-binding spot of parvalbumin (MW = 12,000, pI = 4.9) from human, monkey, rat, mouse, chicken, and fish by immunobinding (manufacturer's technical information). Western blot analysis of brain tissue from rats and a number of other species shows that the rabbit anti-GluR1 antibody used in the present study produces a single band at ~106 kDa comigrating with GluR1 expressed in transfected cells—no cross-reaction occurs with GluR2–4 (manufacturer's technical information). Similarly, the polyclonal anti-GluR2 antibody recognizes a single band at 108 kDa on Western blots of rat brain—it does not cross-

react with GluR1, 3, or 4 (manufacturer's technical information). The polyclonal anti-GluR4 antibody recognizes a single band at 108 kDa on Western blots of rat brain—it does not cross-react with GluR1–3 (manufacturer's technical information). Finally, the polyclonal anti-GluR2/3 antibody recognizes a single band at 110 kDa on Western blots of rat brain—it does not cross-react with GluR1 or 4 (manufacturer's technical information).

Following incubation with the primary antibodies described above, cat brain sections were rinsed 4×10 minutes with 0.01 M PB. Cocktails of the secondary antibodies were then added to the sections and allowed to react for 4 hours at room temperature with agitation. The secondary antibodies were all obtained from Molecular Probes and were highly cross-absorbed anti-rabbit IgG or anti-mouse IgG tagged with AlexaFluor 488 or AlexaFluor 555. The AlexaFluor 555 and AlexaFluor 488 goat anti-mouse IgGs (catalog #A-21424 and A-11029) were both prepared from affinity-purified antibodies that react with IgG heavy chains and all classes of immunoglobulin light chains from mouse. The AlexaFluor 555 and AlexaFluor 488 goat anti-rabbit IgG (catalog #A-21429 and A-11034) was prepared from affinity-purified antibodies that react with IgG heavy chains and all classes of immunoglobulin light chains from rabbit. To minimize cross-reactivity, all secondary antibodies used in the present double-labeling study were highly cross-absorbed: the anti-mouse antibodies were reacted against bovine IgG, rat IgG, rabbit IgG, goat IgG, human IgG, and human serum, whereas the anti-rabbit antibodies were treated against bovine IgG, rat IgG, mouse IgG, goat IgG, and human IgG (manufacturer's technical information).

After incubation with the secondary antibodies, sections were rinsed one final time. They were then mounted on glass slides, coverslipped with Vectashield antifading mounting medium (Vector, Burlingame, CA), and viewed by using an Olympus AX70 fluorescence microscope. All photomicrographs presented in the results section were captured by using a high-sensitivity/high-resolution video camera, interfaced with a PC running ImagePro software, which was used for the quantitative analysis.

The cellular distribution and pattern of staining obtained with the Sigma anti-calbindin and anti-parvalbumin antibodies were identical to those previously published by our laboratory (Huxlin and Pasternak, 2001) and several others (Alcantara and Ferrer, 1994; Hogan and Berman, 1993, 1994) for cat visual cortex. Several groups have previously demonstrated the specificity of these same antibodies in cat brain, either by preabsorbing them with purified calbindin/parvalbumin and demonstrating absence of staining (Hogan and Berman, 1993), or by performing Western blot analysis (Hogan and Berman, 1994). Chen and colleagues (2000) performed a Western blot analysis on the polyclonal anti-NMDAR1 antibody from Chemicon by using cat visual cortical tissue and demonstrated that the antibody labels a single band at the appropriate molecular weight (120 kDa).

Specificity of the polyclonal anti-GluR2 antibody from Chemicon was also verified on cat visual cortical tissue by Van Damme and colleagues (2003), who showed it to label a single band at ~108 kDa. The immunostaining obtained in the present study with antibodies against AMPA receptor subunits GluR1–4 was consistent with all previous reports for such antibody staining in cat visual cortex (Gutierrez-Igarza et al., 1996; Van Damme et al., 2003). Indeed, Gutierrez-Igara and colleagues (1996) found considerable homology in molecular composition and size between the AMPA receptor GluR1–4 subunits in cat and rat brain.

Finally, several control reactions were performed on our cat brain sections, whereby the primary antibodies were omitted from the immunoreactions. This resulted in a total lack of cellular staining.

Quantitative immunohistochemical analysis

Selecting cortical locations for analysis—Because electrophysiological mapping of area 18 would have caused tissue damage and associated alterations in the neurochemistry of cortical layers we needed to analyze, published electrophysiological maps (Tusa et al., 1979, 1981) were used to estimate retinotopy for brain regions directly exposed to visual retraining following LS lesions. For Cat 1, retraining was carried out by using a circular stimulus 5° in diameter, at ~9° eccentricity in the lower left visual quadrant ("a" in Fig. 3A and Fig. 4A). Following recovery of direction range thresholds at this location, performance in Cat 1's upper left quadrant was still abnormal (Huxlin and Pasternak, 2004; Fig. 2B). Therefore, for Cat 1, neurochemical changes in portions of area 18 where the retrained lower visual quadrant was represented (1–3 mm anterior to the interaural line) were compared with those in which the untrained, upper visual quadrant was represented (7–11 mm posterior to the interaural line; see schematic illustration in Fig. 4D).

Cat 2 underwent retraining with a stimulus 4° in diameter in the far (~20° eccentricity) upper left visual quadrant ("b" in Fig. 3A and Fig. 4B). Thus, as shown in Figure 4E, neurochemical expression in portions of area 18 where the retrained far upper quadrant was represented (ventral third of area 18 between 9 and 10.2 mm posterior to the interaural line) was compared with that in parts of area 18 in which untrained portions of the visual field were represented (dorsal two-thirds of area 18 between 9 and 10.2 mm posterior to the interaural line and portions of area 18 anterior to the interaural line).

Cat 3 underwent retraining with a stimulus 4° in diameter in the far (~20° eccentricity) lower right visual quadrant ("c" in Fig. 3A and Fig. 4C). Neurochemical expression in portions of area 18 in which the retrained far lower quadrant was represented (between 4 and 8 mm anterior to the interaural line) was compared with expression in parts of area 18 in which untrained portions of the visual field were represented (lower third of area 18 between 7 and 8 mm posterior to the interaural line; Fig. 4F).

The fact that the retrained brain region of Cats 1 and 3 corresponded approximately to the untrained brain region of Cat 2, and vice versa, provided an excellent control for potential differences in GluR receptor subunit expression between upper and lower visual field representations in area 18. Finally, the regions of area 18 selected for analysis in control animals (Cats 4–9) were identical to those analyzed in Cats 1–3.

Estimating the proportion of double-labeled cells—In order to assess what proportion of LS-projecting pyramidal cells, parvalbumin-positive interneurons, and calbindin-positive interneurons expressed GluR1, GluR2, GluR2/3, GluR4, and NR1, pairs of images of layers II and III of area 18 were captured by using a 40× objective in each coronal brain section of interest. For each cortical location, a first image was collected under fluorescein illumination by using ImagePro software. The filter was then changed to rhodamine illumination, and a second image was collected at the same location and focal plane. All DiI-, calbindin-, or parvalbumin-positive cells in the field of view were tagged first. The tags were saved and superposed onto the second image containing the double label (one of the glutamate receptor subunits). The number of cells containing both labels was then calculated as a proportion of the number of DiI-, calbindin-, or parvalbumin-positive cells for each pair of images. Between 74 and 1,206 cells (mean = 446 cells) were analyzed from at least two brain sections, from at least two different animals for each of the three cell types of interest (DiI-, calbindin-, and parvalbumin-positive cells) in each of the treatment categories. The two-tailed Student's t-test was used to measure statistical significance, with $P < 0.05$ as the criterion.

Photographs of the labeled cells were captured through an Olympus AX70 fluorescence microscope by using a high-sensitivity/high-resolution video camera, interfaced with a PC

running ImagePro software. Images were collected in ImagePro, saved in TIFF format, and imported into Power-point, where they were resized and cropped to generate the layout in Figure 6 and Figure 7. Contrast and brightness were manipulated only minimally in order to normalize the background across the different images. Figure 6 and Figure 7 were then resaved in TIFF format and imported into Adobe Photoshop (San Jose, CA), by means of which red was changed to magenta to generate the final images.

RESULTS

Extent of LS cortical lesions

Analysis of serial brain sections reacted for CO activity confirmed that all cats with ibotenic acid injections into LS cortex (Cats 1–6) exhibited contiguous damage to the gray matter on the banks of the LS sulcus, with no islands of spared tissue (Fig. 5). By registration with published retinotopic maps (Palmer et al., 1978;Tusa et al., 1981), it was determined that the posteromedial and posterolateral lateral suprasylvian visual area (PMLS and PLLS), which are critical for complex visual motion perception, were completely destroyed in all cats, as was much of surrounding areas 21a, 7, the dorsal lateral suprasylvian visual area (DLS), the ventral lateral suprasylvian visual area (VLS), and the anteromedial and anterolateral lateral suprasylvian visual areas (AMLS and ALLS) (Fig. 5). Importantly, area 18, the subject of the present analysis, was completely undamaged by the lesions. Area 17, most of area 19, and the anterior ectosylvian visual area (AEV), which are normally interconnected with LS cortex (Fig. 1), were also intact (Fig. 5).

Distribution of the three cell types of interest in area 18

LS-projecting pyramidal cells retrogradely labeled with DiI were located in layers II and III of areas 17, 18, and 19 (Fig. 6A–F) and in layer V of AEV (not shown). The fact that numerous DiI-labeled cells were observed in early visual areas many months after an ipsilateral lesion of LS cortex suggests that a significant proportion of LS-projecting cells survive over the long term following lesion of the adult LS cortex.

Cats with intact LS cortex and cats with LS lesions displayed a concentration of calbindin-positive cells in layers II–III (Fig. 6G) and a uniform distribution of parvalbumin-positive cells across layers II–VI of area 18 (Fig. 6J), as previously reported (Baimbridge et al., 1992;Hof et al., 1999;Huxlin and Pasternak, 2001). Calbindin- and parvalbumin-positive cells were never labeled with DiI (Figs. 6G–L), nor were the two calcium-binding proteins ever colocalized within individual cells. Thus, LS-projecting, calbindin- and parvalbumin-positive cells represent three adjacent, likely interconnected, but non-overlapping cell populations within corticocortical projection layers of area 18.

Effect of LS lesions on AMPA receptor subunit expression in area 18

LS-projecting pyramidal cells—In normal (intact) cats, over 95% of LS-projecting pyramidal cells in layers II and III of area 18 expressed all four subunits of the AMPA receptor (Fig. 7A–C, Table 1). Following LS lesions and in the presence of normal visual experience (but not intensive visual retraining), nearly 20% of LS-projecting cells no longer expressed GluR1 ($P = 0.003$), and ~5% no longer expressed GluR4 ($P = 0.018$) at levels detectable with immunohistochemistry, although expression of GluR2 and GluR2/3 remained unchanged (Table 1).

Interneurons—In normal cats, on average, ~96% of parvalbumin- and calbindin-positive interneurons in layers II and III of area 18 expressed all four subunits of the AMPA receptor (Fig. 7D–I, Table 1). Following LS lesions, 13, 22, 12, and 17% of calbindin-positive cells in layers II/III of area 18 no longer expressed GluR1, 2, 2/3, or 4, respectively, at levels detectable

with immunohistochemistry (Table 1). The proportion of parvalbumin-positive cells expressing GluR2 and GluR2/3 also fell by 16 and 30%, respectively ($P = 0.003$ and $P = 0.0005$, respectively), although there was no significant change in the proportion of parvalbumin-positive cells expressing GluR1 and 4 (Table 1).

Cell-type-specific restoration of AMPAR subunit expression in retrained cats

When retrained portions of the ipsilesional area 18 ("a", "b," and "c" in Fig. 3 and Fig 4) were analyzed for cell-type-specific expression of AMPAR subunits, $98 \pm 0.9\%$ and $99 \pm 0.4\%$ of LS-projecting pyramidal cells expressed GluR1 and 4, respectively (Table 1). This was not significantly different from expression levels in normal, nonlesioned cats and was accompanied by a return to normal expression levels of all AMPA receptor subunits in calbindin- and parvalbumin-positive cells (Table 1).

Retinotopic specificity of restored AMPAR subunit expression in retrained cats

To assess the retinotopic specificity of the training-induced increases in AMPA receptor subunit expression, we analyzed regions of the ipsilesional area 18 in retrained cats (1, 2, and 3) that represented visual field locations not exposed to retraining. These regions were not visually deprived, experiencing normal vision post lesion.

Only $85 \pm 3.4\%$ and $93 \pm 2\%$ of LS-projecting pyramidal cells in untrained regions of area 18 in Cats 2 and 3 expressed GluR1 and 4 respectively, values that were not significantly different from percentages obtained in Cats 4–6, which were not behaviorally trained (Table 1).

Similarly, in calbindin-positive interneurons, the "normalization" of AMPAR subunit expression did not extend beyond regions of area 18 exposed to retraining. (The percentage of calbindin-positive cells remained significantly below normal in untrained portions of area 18; Table 1.) However, for parvalbumin-positive interneurons, the return to normal GluR2 and 2/3 expression occurred in both trained and untrained portions of the ipsilesional area 18 (Table 1).

Hemispheric specificity of restored AMPAR subunit expression in retrained cats

As an additional control for the hemisphere specificity of training-induced changes in AMPAR subunit expression, the proportion of calbindin- and parvalbumin-positive cells in layers II and III of area 18 was quantified in the intact (contralesional) hemispheres of Cats 1–3. Calbindin- and parvalbumin-positive cells in the contralesional hemispheres exhibited depressed AMPAR subunit expression similar to that seen ipsilateral to the LS lesion (bold values in Table 1). This suggests a bilateral effect of unilateral LS lesions on the visual cortical circuitry, which was not reversed following intensive visual retraining administered to the damaged hemispheres, even in the case of parvalbumin-positive cells.

Effect of LS lesions and retraining on NMDAR1 expression

In addition to their expression of AMPA receptor subunits, $98 \pm 2.3\%$ of LS-projecting, $95 \pm 1\%$ of calbindin-positive, and $94 \pm 0.6\%$ of parvalbumin-positive cells in supragranular layers of area 18 in nonlesioned, control cats expressed the NR1 subunit of the NMDA receptor (Fig. 7J–L, Table 1). Given that the NR1 subunit is obligatory for functional NMDA receptors, these results suggest that the great majority of cells examined probably expressed functional NMDA receptors in addition to AMPA receptors. However, in contrast to their effect on AMPA receptor subunits, neither LS lesions nor postoperative behavioral experience (whether this was normal visual experience or intensive visual retraining) significantly altered expression of NR1 in our three cell types of interest (Table 1).

DISCUSSION

In adult mammals with highly developed visual systems, visual cortical damage causes specific losses in visual perception. In most cases, spontaneous, rapid perceptual improvements occur (e.g. Yamasaki and Wurtz, 1991), which are likely due to resolving inflammation and limited reorganization around the lesion site (Cauraugh and Summers, 2005). Once spontaneous improvements have stabilized, however, residual visual deficits are usually considered permanent (Taub et al., 2002). In normal subjects, practice on visual tasks can significantly improve visual perception and alter neuronal function within both high- and low-level visual cortical areas (Newsome and Paré, 1988; Gilbert et al., 2001; Schoups et al., 2001; Salazar et al., 2004). We and others have also found beneficial effects of visual training on perception after lesions of extrastriate visual cortex, especially areas MT/MST in primates (Rudolph and Pasternak, 1999) and LS cortex in cats (Rudolph and Pasternak, 1996; Huxlin and Pasternak, 2004).

However, the cellular mechanisms by which training induces visual recovery in the damaged adult visual system, and the identity of visual areas that contribute to this recovery, remain largely unknown. Because training-induced improvements in motion perception after LS lesions in the cat were retinotopically restricted to visual field locations exposed to intensive training post lesion (Huxlin and Pasternak, 2004), we hypothesized that early visual cortical areas, which are known to possess smaller receptive fields and tighter retinotopy (Tusa et al., 1981), were likely to have contributed significantly to the observed recovery. In the present study, changes in the expression of AMPAR subunits were used as cellular indicators of circuitry-wide changes in activity levels. By comparing expression of GluR1–4 in normal (intact) cats, cats with LS lesions but no training, and cats with LS lesions plus visual training at a single, retinotopic location, we showed that area 18, an early visual cortical area in the cat with strong connectivity to LS cortex and a demonstrated role in visual motion processing, exhibits cell-type-specific, long-term downregulation of AMPA receptor subunit expression following damage to LS cortex. Most importantly, intensive visual retraining post lesion reversed these changes in a cell-type-specific and, in some cases, retinotopically specific manner.

Expression of AMPA receptor subunits in supragranular layers of area 18 of normal cats

Previous reports in rodents (Geiger et al., 1995; Vissavajjhala et al., 1996; Angulo et al., 1997; Kondo et al., 1997) and primates (Vickers et al., 1993; Munoz et al., 1999) suggest that some classes of cortical neurons, including those expressing calcium-binding proteins, can be differentiated by their expression of different AMPA receptor subunits. However, our present experiments revealed that in normal cats, the great majority of calbindin- and parvalbumin-positive cells, and the majority of LS-projecting pyramidal cells in layer II/III of area 18 expressed all four subunits of the AMPA receptor. The fact that > 95% of these neurons expressed each of the glutamate receptor subunits tested makes it likely that they coexpressed these different subunits. The discrepancy between our results and those reported previously in other species may be due to simple species differences or to the fact that we restricted our analysis to three specific cell types within supragranular layers II and III of a single visual area: area 18. Nevertheless, our data were highly consistent between cats and showed further that in addition to their expression of GluR1–4, the great majority of the three cell types examined also expressed the NR1 subunit of the NMDA receptor. Such coexpression at the protein level implies at the very least, *a capacity* of LS-projecting pyramidal cells and calbindin- and parvalbumin-positive interneurons to express both functional AMPA and NMDA receptors on their cell surface, as noted in several other types of adult neurons (Jones and Baughman, 1991; Kharazia et al., 1996).

Unilateral LS lesions cause bilateral decreases in AMPA receptor subunit expression in layers II/III of area 18

Our earlier study (Huxlin and Pasternak, 2001) showed that many months after a lesion of LS cortex, calbindin-positive interneurons in supragranular layers of the area 18 continued to exhibit signs of downregulated activity. This effect was significantly more pronounced in area 18 than in areas 17 and 19 and affected calbindin-positive cells to a larger degree than parvalbumin-positive cells (Huxlin and Pasternak, 2004). This is consistent with electrophysiological studies, which show that when higher level visual cortical areas are temporarily inactivated, cortical neurons at earlier levels of the visual system exhibit a decrease in the amplitude of their responses to stimulation (Hupe et al., 1998; Wang et al., 2000; Galuske et al., 2002; Bardy et al., 2006). This suggests that the major influence of feedback projections on early visual neurons is excitatory in nature. Over the long term, a persistent lack of excitatory feedback from higher level visual cortex might permanently depress the activity of lower level visual cortical neurons.

A further, relevant observation is that when they do not kill cells, persistent decreases in neuronal excitability are known to be associated with changes in the sensitivity and subunit composition of AMPA and NMDA receptors (Tighilet et al., 1998; Alvarez et al., 2000; Brown et al., 2004). And indeed, the present experiments showed that unilateral LS lesions caused ~18% of calbindin-positive cells and 24% of parvalbumin-positive cells in area 18 of *both* hemispheres to decrease their expression of GluR2 and 2/3 below levels detectable with immunohistochemistry. Calbindin- and parvalbumin-positive cells are a class of largely inhibitory cortical interneurons, characterized by their content of high-affinity, calcium-binding proteins (Persechini et al., 1989; Baimbridge et al., 1992; Hof et al., 1999). Taken together, they constitute > 90% of inhibitory interneurons in layers II/III of the cat's area 18 (Huxlin and Pasternak, 2001). That AMPA receptor subunit expression was affected in these two cell types was not totally surprising, given our previous observations in this model system (Huxlin and Pasternak, 2001). What was surprising was the bilateral nature of the downregulation of GluR2 and 2/3 in these interneurons, for two reasons: first, perceptual effects of LS lesions are strictly unilateral (Huxlin and Pasternak, 2004). Second, calbindin- and parvalbumin-positive cells are *interneurons*, which do not normally project between different cortical areas, or across the callosum. Our working hypothesis is that these cells were affected in an indirect manner, because of the relatively extensive transcallosal connectivity of higher level visual cortical areas, including LS cortex (Segraves and Rosenquist, 1982a,b).

A loss of expression of GluR2 and 2/3 in ~20% of calbindin- and parvalbumin-positive cells most likely signifies that these cells are no longer synthesizing GluR2 and/or 3 in detectable quantities. If fewer GluR2 subunits are made, fewer or no GluR2 subunits may be incorporated into synaptic AMPA receptors. AMPA receptors with a low GluR2 component are characterized by increased Ca^{2+} permeability (Bochet et al., 1994; Jonas et al., 1994; Geiger et al., 1995; Jonas and Burnashev, 1995). If the loss of bidirectional interactions between area 18 and LS cortex causes a generalized decrease in neuronal activity within supragranular layers of area 18, a long-term increase in Ca^{2+} permeability may represent a survival mechanism for interneurons containing high-affinity calcium-binding proteins and thus, high calcium-buffering capacity (Bennett and Huxlin, 1996).

Furthermore, consistent with their greater sensitivity to LS lesions (Huxlin and Pasternak, 2001), calbindin-positive cells, unlike parvalbumin-positive cells, also exhibited changes in their expression of GluR1 and GluR4 subunits. If expression of all four AMPA receptor subunits decreased in the same cells, but the cells continued to express NR1 (as was the case for all three cell types of interest in the present study), this may reflect the appearance of silent synapses (possessing NMDA but not AMPA receptors; Isaac et al., 1995; Liao et al., 1995; Durand et al., 1996), another phenomenon that might be consistent with a lesion-induced

downregulation in cellular excitability (Isaac et al., 1995; Liao et al., 1995; Durand et al., 1996).

As might be expected, loss of their major cortical target also affected excitatory, LS-projecting pyramidal cells in supragranular layers of area 18. A large number of DiIabeled, LS-projecting pyramidal cells were still present in layers II/III of early visual areas, including area 18, many months after the lesion. However, 20% of these cells no longer expressed GluR1. About 5% of them also lost expression of GluR4 to below levels detectable by immunohistochemistry. However, a normal proportion of LS-projecting cells continued to express GluR2 and GluR2/3, a marked contrast from the behavior of surrounding calbindin- and parvalbumin-positive interneurons. GluR1 is important for activity-, NMDA receptor-, and CaMKII-driven exocytosis of AMPA receptors to the cell membrane and their subsequent translocation to synaptic sites (Shi et al., 1999; Hayashi, 2000; Passafaro et al., 2001; Song and Huganir, 2002). Decreased GluR1expression means the removal of an important cyclic adenosine monophosphate (cAMP) and protein kinase A (PKA)-regulated, Ca^{2+}-permeable subunit (Keller et al., 1992) from synaptic AMPA receptors, leaving these receptors dominated by GluR2, and thus relatively impermeable to Ca^{2+} (Geiger et al., 1995). Persistent, small, slow elevations in $[Ca^{2+}]_i$ upon cellular activation can ultimately induce long-term depression (LTD) rather than long-term potentiation (LTP) (Bi and Poo, 2001), and this would again be consistent with a lesion-induced downregulation in excitability within upper layers of area 18.

The fact that GluR4 subunit expression might also have decreased in some of the cells that downregulated their expression of GluR1 (both LS-projecting cells and calbindin-positive cells) is also interesting because of the similarities in the tail sequences of these two subunits (for review, see Malinow et al., 2000). Perhaps LS lesions alter the function and/or expression of intracellular proteins that bind to the tail region of both these subunits, thus affecting their expression concurrently.

Finally, LS lesions caused no detectable changes in the expression of NR1 by our three cell types of interest. The relative stability of synaptic NMDA receptors has been previously reported in other systems, in which it contrasts with the activity-dependent cycling of AMPA receptors and their subunits in and out of synaptic zones (Lüscher et al., 1999; Wenthold et al., 2003; Brown et al., 2004). It also proved a useful internal control for the changes observed with regard to the expression of AMPAR subunits in area 18.

Unilateral effect of postlesion visual training on AMPA receptor subunit expression in area 18

Although a relatively small proportion of supragranular neurons in area 18 (5–30%) exhibited changes in AMPA receptor subunit expression, the consistency of these alterations (with regard to cell type *and* subunit affected) provided a reproducible, lesion-induced baseline of neuronal changes against which to contrast the effects of postlesion visual experience. Although inactivation of higher level visual cortex decreases activity in early visual areas, intensive visual stimulation or training is thought to increase activity at both lower levels (Schoups et al., 2001; Eyding et al., 2002; Salazar et al., 2004) and higher levels (Logothetis et al., 1995; Kobatake et al., 1998; Salazar et al., 2004) of the visual cortical hierarchy (but see Ghose et al., 2002). Thus, although LS lesions may decrease expression of some AMPAR subunits in area 18, visual training would be expected to reverse at least some of these changes in a proportion of the affected neurons.

However, the retinotopic specificity of recovery to retrained visual field locations (Huxlin and Pasternak, 2004) allows two further predictions to be made: 1) if the major effect of postlesion training occurred through plasticity of feed-forward pathways terminating in supragranular layers of area 18, then the return to normal AMPA receptor subunit expression should occur

only in portions of area 18 directly exposed to the retraining stimuli; and 2) if the major effect of postlesion training was to stimulate the development or strengthening of feedback projections to area 18, then the return to normal AMPA receptor subunit expression should occur over broader expanses of area 18, including some representation outside the region directly exposed to retraining stimuli. This is because feedback corticocortical projections typically exhibit a much wider retinotopic termination pattern than feed-forward cortical projections (Rockland et al., 1994; Salin and Bullier, 1995).

As previously reported (Huxlin and Pasternak, 2004), localized visual discrimination retraining post lesion improved motion discrimination thresholds at the retrained locations. In addition, it also increased AMPAR subunit expression back to normal levels in all three cell types examined. For LS-projecting and calbindin-positive cells, this normalization was restricted to portions of area 18 corresponding retinotopically to the retrained region of the impaired visual hemifield. This suggests a primary contribution of feed-forward pathways terminating in supragranular layers of area 18 to training-induced visual recovery. It also makes it unlikely that recovery was an artifact caused by the animals learning to interpret light scatter or portions of the stimulus falling within intact portions of their visual field during retraining. Finally, it clearly demonstrates the lack of effectiveness of normal visual experience and of extensive *prelesion* visual training (i.e., cats were overtrained prior to the lesion) for attaining such localized behavioral and neurochemical recovery.

Parvalbumin-positive cells were the only cell type examined in which GluR expression returned to normal *outside* (albeit only in the ipsilesional hemisphere) of the area 18 representation of the retrained locations. The fact that this normalization of GluR expression occurred only in cats retrained after their lesion supports the notion that this is truly an effect of the training. However, why should the spatial distribution of training-induced changes in calbindin- and parvalbumin-positive interneurons be so different? One possible explanation resides in their differing morphologies and connectivity patterns (Defelipe et al., 1990, 1999; Meyer et al., 2002), with some parvalbumin-positive cells forming very long, horizontal connections across cortex (DeFelipe et al., 1989). Another possibility, as proposed earlier, is that visual training induces changes in the feedback input to parvalbumin-positive cells, which in the early visual cortex of rodents are the only type of interneurons known to receive a direct feedback projections from higher level visual cortical areas (Gonchar and Burkhalter, 1999). Because feedback projections generally exhibit broader retinotopy than feed-forward projections (Rockland et al., 1994; Salin and Bullier, 1995), this may explain the broader retinotopy of training-induced changes affecting parvalbumin-positive cells. In cats with LS lesions, potential sources of such feedback input are relatively few and are most likely to include areas 19 and 7 and AEV.

Finally, we should note that although the effects of LS lesions on AMPAR subunit expression in supragranular layers of area 18 were bilateral and persisted for many months, the effects of postlesion visual training on area 18 were strictly unilateral and restricted to the trained (lesioned) hemisphere. Low-level visual cortical areas (17 and 18) exhibit much weaker interhemispheric connections than higher level visual areas (Segraves and Rosenquist, 1982a,b). The fact that training effects were only evident unilaterally further supports the notion that early, rather than higher level, visual cortical areas may be particularly important substrates of training-induced visual recovery after damage to LS cortex.

CONCLUSIONS

Our results provide concrete evidence in an animal model that training-induced recovery of motion perception after extrastriate visual cortical damage in adulthood is associated with specific neurochemical alterations in both excitatory and inhibitory components of a low-level

area in the visual cortical hierarchy. Our experiments show that different cell types are differentially affected both by distant damage to the visual cortical circuitry and by the kind of postlesion training that leads to perceptual improvements. Indeed, the cell-specific molecular alterations presently identified may represent sensitive indicators of large-scale plasticity in adult cortical circuits. Our data further reinforce the notion that the mature visual cortical system of large-brained mammals is capable of significant functional plasticity after damage. However, they also highlight the critical importance and effectiveness of targeted, intensive visual retraining for recruiting a level of visual system plasticity that is able to mediate functional recovery after such damage.

Acknowledgments

LITERATURE CITED

Akase E, Inokawa H, Toyama K. Neuronal responsiveness to three-dimensional motion in cat posteromedial lateral suprasylvian cortex. Exp Brain Res 1998;122:214–226. [PubMed: 9776520]

Alcantara S, Ferrer I. Postnatal development of parvalbumin immunoreactivity in the cerebral cortex of the cat. J Comp Neurol 1994;348:133–149. [PubMed: 7814682]

Alvarez FJ, Fyffe REW, Dewey DE, Haftel VK, Cope TC. Factors regulating AMPA-type glutamate receptor subunit changes induced by sciatic nerve injury in rats. J Comp Neurol 2000;426:229–242. [PubMed: 10982465]

Angulo MC, Lambolez B, Audinat E, Hestrin S, Rossier J. Subunit composition, kinetic and permeation properties of AMPA receptors in single neocortical nonpyramidal cells. J Neurosci 1997;17:6685–6696. [PubMed: 9254681]

Baimbridge KG, Celio MR, Rogers JH. Calcium-binding proteins in the nervous system. Trends Neurosci 1992;15:303–308. [PubMed: 1384200]

Bardy C, Huang JY, Wang C, Fitzgibbon T, Dreher B. 'Simplification' of responses of complex cells in cat striate cortex: suppressive surrounds and 'feedback' inactivation. J Physiol 2006;574:731–750. [PubMed: 16709635]

Bear MF, Rittenhouse CD. Molecular basis for induction of ocular dominance plasticity. J Neurobiol 1999;41:83–91. [PubMed: 10504195]

Bennett MR, Huxlin KR. Neuronal cell death in the mammalian nervous system: the Calmortin hypothesis. Gen Pharmacol 1996;27:407–419. [PubMed: 8723518]

Bi G, Poo M. Synaptic modification by correlated activity: Hebb's postulate revisited. Annu Rev Neurosci 2001;24:139–166. [PubMed: 11283308]

Bochet P, Audinat E, Lambolez B, Crepel F, Rossier J, Iino M, Tsuzuki K, Ozawa S. Subunit composition at the single cell level explains functional properties of a glutamate-gated channel. Neuron 1994;12:383–388. [PubMed: 7509161]

Bredt DS, Nicoll RA. AMPA receptor trafficking at excitatory synapses. Neuron 2003;40:361–379. [PubMed: 14556714]

Brown KM, Wrathall JR, Yasuda RP, Wolfe BB. Glutamate receptor subunit expression after spinal cord injury in young rats. Dev Brain Res 2004;152:61–68. [PubMed: 15283995]

Carmignoto G, Vicini S. Activity-dependent decrease in NMDA receptor responses during development of the visual cortex. Science 1992;258:1007–1011. [PubMed: 1279803]

Carroll RC, Zukin RS. NMDA-receptor trafficking and targeting: implications for synpatic transmission and plasticity. Trends Neurosci 2002;25:571–577. [PubMed: 12392932]

Cauraugh JH, Summers JJ. Neural plasticity and bilateral movements: a rehabilitation approach for chronic stroke. Prog Neurobiol 2005;75:309–320. [PubMed: 15885874]

Chen L, Cooper NGF, Mower GD. Developmental changes in the expression of NMDA receptor subunits (NR1, NR2A, NR2B) in the cat visual cortex and the effects of dark rearing. Mol Brain Res 2000;78:196–200. [PubMed: 10891601]

Collingridge GL, Singer W. Excitatory amino acid receptors and synaptic plasticity. Trends Pharmacol Sci 1990;11:290–296. [PubMed: 2167544]

DeFelipe J, Hendry SHC, Jones EG. Visualisation of chandelier cell axons by parvalbumin immunoreactivity in monkey cerebral cortex. Proc Natl Acad Sci U S A 1989;86:2093–2097. [PubMed: 2648389]

DeFelipe J, Hendry SHC, Hashikawa T, Molinari M, Jones EG. A microcolumnar structure of monkey cerebral cortex revealed by immunocytochemical studies of double-bouquet cell axons. Neuroscience 1990;37:655–673. [PubMed: 1701039]

Defelipe J, Gonzalez-Albo MC, Del Rio MR, Elston GN. Distribution and patterns of connectivity of interneurons containing calbindin, calretinin, and parvalbumin in visual areas of the occipital and temporal lobes of the macaque monkey. J Comp Neurol 1999;412:515–526. [PubMed: 10441237]

Dreher B, Wang C, Turlejski KJ, Djavadian RL, Burke W. Areas PMLS and 21a of cat visual cortex: two functionally distinct areas. Cereb Cortex 1996;6:585–599. [PubMed: 8670684]

Durand GM, Kovalchuk Y, Konnerth A. Long-term potentiation and functional synapse induction in developing hippocampus. Nature 1996;381:71–75. [PubMed: 8609991]

Ehrlich I, Malinow R. Postsynaptic density 95 controls AMPA receptor incorporation during long-term potentiation and experience-driven synaptic plasticity. J Neurosci 2004;24:916–927. [PubMed: 14749436]

Eyding D, Schweigart G, Eysel UT. Spatio-temporal plasticity of cortical receptive fields in response to repetitive visual stimulation in the adult cat. Neuroscience 2002;112:195–215. [PubMed: 12044484]

Fox K, Daw NW. Do NMDA receptors have a critical function in visual cortical plasticity? Trends Neurosci 1993;16:116. [PubMed: 7681235]

Fox K, Sato H, Daw N. The location and function of NMDA receptors in cat and kitten visual cortex. J Neurosci 1989;9:2443–2454. [PubMed: 2568409]

Fox K, Daw N, Sato H, Czepita D. The effect of visual experience on development of NMDA receptor synaptic transmission in kitten visual cortex. J Neurosci 1992;12:2672–2684. [PubMed: 1351937]

Galuske RAW, Schmidt KE, Goebel R, Lomber SG, Payne BR. The role of feedback in shaping neural representations in cat visual cortex. Proc Natl Acad Sci U S A 2002;99:17083–17088. [PubMed: 12477930]

Geiger JR, Melcher T, Koh DS, Sakmann B, Seeburg PH, Jonas P, Moyner H. Relative abundance of subunit mRNAs determines gating and Ca2+ permeability of AMPA receptors in principal neurons and interneurons in rat CNS. Neuron 1995;15:193–204. [PubMed: 7619522]

Ghose GM, Yang T, Maunsell JH. Physiological correlates of perceptual learning in monkey V1 and V2. J Neurophysiol 2002;87:1867–1888. [PubMed: 11929908]

Gilbert CD, Das A, Ito M, Kapadia MK, Westheimer G. Cortical dynamics and visual perception. Cold Spring Harbor Symp Quant Biol 1996;61:105–113. [PubMed: 9246440]

Gilbert CD, Sigman M, Crist RE. The neural basis of perceptual learning. Neuron 2001;31:681–697. [PubMed: 11567610]

Gonchar Y, Burkhalter A. Differential subcellular localization of forward and feedback inter-areal inputs to parvalbumin expressing GABAergic neurons in rat cortex. J Comp Neurol 1999;406:346–360. [PubMed: 10102500]

Gordon B, Pardo D, Conant K. Laminar distribution of MK-801 kainate, AMPA, and muscimol binding sites in cat visual cortex—a developmental study. J Comp Neurol 1996;365:466–478. [PubMed: 8822182]

Grant S, Shipp S. Visuotopic organization of the lateral suprasylvian area and of an adjacent area of the ectosylvian gyrus of cat cortex: a physiological and connectional study. Vis Neurosci 1991;6:315–338. [PubMed: 1711891]

Gutierrez-Igarza K, Fogarty DJ, Perez-Cerda F, Donate-Oliver F, Albus K, Matute C. Localization of AMPA-selective glutamate receptor subunits in the adult cat visual cortex. Vis Neurosci 1996;13:61–72. [PubMed: 8730990]

Hallett M. Plasticity of the human motor cortex and recovery from stroke. Brain Res Rev 2001;36:169–174. [PubMed: 11690613]

Hayashi Y. Driving AMPA receptors into synapses by LTP and CaMJII: requirement for GluR1 and PDZ domain interaction. Science 2000;287:2262–2267. [PubMed: 10731148]

Hof PR, Glezer II, Conde F, Flagg RA, Rubin MB, Nimchinsky EA, Weisenhorn DMV. Cellular distribution of the calcium-binding proteins parvalbumin, calbindin, and calretinin in the neocortex of mammals: phylogenetic and developmental patterns. J Chem Neuroanat 1999;16:77–116. [PubMed: 10223310]

Hogan D, Berman NEJ. Transient expression of calbindin-D immunoreactivity in layer V pyramidal neurons during postnatal development of kitten cortical areas. Dev Brain Res 1993;74:177–192. [PubMed: 8403381]

Hogan D, Berman NEJ. The development of parvalbumin and calbindin-D28K immunoreactive interneurons in kitten visual cortical areas. Dev Brain Res 1994;77:1–21. [PubMed: 8131257]

Honig MG, Hume RI. Fluorescent carbocyanine dyes allow living neurons of identified origin to be studied in long term cultures. J Cell Biol 1986;103:171–187. [PubMed: 2424918]

Honig MG, Hume RI. DiI and DiO: versatile fluorescent dyes for neuronal labelling and pathway tracing. Trends Neurosci 1989;12:333–335. [PubMed: 2480673]

Hupe JM, James AC, Payne BR, Lomber SG, Girard P, Bullier J. Cortical feedback improves discrimination between figure and background by V1, V2 and V3 neurons. Nature 1998;394:784–787. [PubMed: 9723617]

Huxlin KR, Pasternak T. Long-term neurochemical changes after visual cortical lesions in the adult cat. J Comp Neurol 2001;429:221–241. [PubMed: 11116216]

Huxlin KR, Pasternak T. Training-induced recovery of visual motion perception after extrastriate cortical damage in the adult cat. Cereb Cortex 2004;14:81–90. [PubMed: 14654459]

Isaac JTR, Nicoll RA, Malenka RC. Evidence for silent synapses: implications for the expression of LTP. Neuron 1995;15:427–434. [PubMed: 7646894]

Jonas P, Burnashev N. Molecular mechanisms controlling calcium entry through AMPA-type glutamate receptor channels. Neuron 1995;15:987–990. [PubMed: 7576666]

Jonas P, Racca C, Sakmann B, Seeburg PH, Moyner H. Differences in Ca2+ permeability of AMPA-type glutamate receptor channels in neocortical neurons caused by differential GluR-B subunit expression. Neuron 1994;12:1281–1289. [PubMed: 8011338]

Jones KA, Baughman RW. Both NMDA and non-NMDA subtypes of glutamate receptor are concentrated at synapses on cerebral cortical neurons in culture. Neuron 1991;7:593–603. [PubMed: 1718334]

Kaas JH. Neurobiology: how cortex reorganizes. Nature 1995;375:735–736. [PubMed: 7596403]

Keller BU, Hollmann M, Heinemann S, Konnerth A. Calcium-influx through subunits GluR1/GluR3 of kainate/AMPA receptor channels is regulated by cAMP dependent protein kinase. EMBO J 1992;11:891–896. [PubMed: 1372254]

Kharazia VN, Phend KD, Rustioni A, Weinberg RJ. EM colocalization of AMPA and NMDA receptor subunits at synapses in rat cerebral cortex. Neurosci Lett 1996;210:37–40. [PubMed: 8762186]

Kobatake E, Wang G, Tanaka K. Effects of shape-discrimination training on the selectivity of inferotemporal cells in adult monkeys. J Neurophysiol 1998;80:324–330. [PubMed: 9658053]

Kondo M, Sumino R, Okado H. Combinations of AMPA subunit expression in individual cortical neurons correlate with expression of specific calcium-binding proteins. J Neurosci 1997;17:1570–1581. [PubMed: 9030617]

Kuffler DP. Long-term survival and sprouting in culture by motor-neurons isolated from the spinal cord of adult frogs. J Comp Neurol 1990;302:729–738. [PubMed: 1707066]

Lee C, Weyand TG, Malpeli JG. Thalamic control of cat lateral suprasylvian visual area—relation to patchy association projections from area 18. Vis Neurosci 1998;15:15–25. [PubMed: 9456501]

Liao D, Hessler NA, Malinow R. Activation of postsynaptically silent synapses during pairing-induced LTP in CA1 region of hippocampal slice. Nature 1995;375:400–404. [PubMed: 7760933]

Liao D, Zhang X, O'Brien R, Huganir RL. Regulation of morphological postsynaptic silent synapses in developing hippocampal neurons. Nat Neurosci 1999;2:37–43. [PubMed: 10195178]

Liu S-QJ, Cull-Candy SG. Synaptic activity at calcium-permeable AMPA receptors induces a switch in receptor subtype. Nature 2000;405:454–458. [PubMed: 10839540]

Logothetis NK, Pauls J, Poggio T. Shape representation in the inferior temporal cortex of monkeys. Curr Biol 1995;5:552–563. [PubMed: 7583105]

Lu W, Constantine-Paton M. Eye opening rapidly induces synaptic potentiation and refinement. Neuron 2004;43:237–249. [PubMed: 15260959]

Lüscher C, Xia H, Beattie EC, Carroll RC, von Zastrow M, Malenka RC, Nicoll RA. Role of AMPA receptor cycling in synaptic transmission and plasticity. Neuron 1999;24:649–658. [PubMed: 10595516]

Malenka RC, Nicoll RA. NMDA-receptor-dependent synaptic plasticity—multiple forms and mechanisms. Trends Neurosci 1993;16:521–527. [PubMed: 7509523]

Malinow R, Malenka RC. AMPA receptor trafficking and synaptic plasticity. Annu Rev Neurosci 2002;25:103–126. [PubMed: 12052905]

Malinow R, Mainen ZF, Hayashi Y. LTP mechanisms: from silence to four-lane traffic. Curr Opin Neurobiol 2000;10:352–357. [PubMed: 10851179]

Meyer AH, Katona I, Blatow M, Rozov A, Moyner H. In vivo labeling of parvalbumin-positive interneurons and analysis of electrical coupling in identified neurons. J Neurosci 2002;22:7055–7064. [PubMed: 12177202]

Munoz A, Woods TM, Jones EG. Laminar and cellular distribution of AMPA, kainate and NMDA receptor subunits in monkey sensory-motor cortex. J Comp Neurol 1999;407:472–490. [PubMed: 10235640]

Newsome WT, Paré EB. A selective impairment of motion perception following lesions of the middle temporal visual area (MT). J Neurosci 1988;8:2201–2211. [PubMed: 3385495]

Palmer LA, Rosenquist AC, Tusa RJ. The retinotopic organization of lateral suprasylvian visual areas in the cat. J Comp Neurol 1978;177:237–256. [PubMed: 621290]

Passafaro M, Piéch V, Sheng M. Subunit-specific temporal and spatial patterns of AMPA receptor exocytosis in hippocampal neurons. Nat Neurosci 2001;4:917–926. [PubMed: 11528423]

Payne BR. Evidence for visual cortical area homologs in cat and macaque monkey. Cereb Cortex 1993;3:1–25. [PubMed: 8439738]

Persechini A, Moncrief ND, Kretsinger RH. The EF-hand family of calcium-modulated proteins. Trends Neurosci 1989;12:462–467. [PubMed: 2479149]

Petralia RS, Esteban JA, Wang Y-X, Partridge JG, Zhao H-M, Wenthold RJ. Selective acquisition of AMPA receptors over postnatal development suggests a molecular basis for silent synapses. Nat Neurosci 1999;2:31–36. [PubMed: 10195177]

Price TA, Huxlin KR. Differential effect of adult cortical lesions on Glu receptor expression in projection cells and interneurons of the afferent circuitry. Soc Neurosci Abstr. 2001

Rauschecker, JP. Visual function of the cat's LP/LS subsystem in global motion processing. In: Hicks, TP.; Benedek, G., editors. Progress in brain research. Amsterdam: Elsevier; 1988. p. 95-108.

Remmel RS. An inexpensive eye movement monitor using the scieral search coil technique. IEEE Trans Biomed Eng BME 1984;31:388–390.

Rockland KS, Saleem KS, Tanaka K. Divergent feedback connections from areas V4 and TEO in the macaque. Vis Neurosci 1994;11:579–600. [PubMed: 8038130]

Rudolph KK, Pasternak T. Lesions in cat lateral suprasylvian cortex affect the perception of complex motion. Cereb Cortex 1996;6:814–822. [PubMed: 8922338]

Rudolph K, Pasternak T. Transient and permanent deficits in motion perception after lesions of cortical areas MT and MST in the macaque monkey. Cereb Cortex 1999;9:90–100. [PubMed: 10022498]

Rumpel S, Hatt H, Gottmann K. Silent synapses in the developing rat visual cortex: evidence for post-synaptic expression of synaptic plasticity. J Neurosci 1998;18:8863–8874. [PubMed: 9786992]

Salazar RF, Kayser C, König P. Effects of training on neural activity and interactions in primary and higher visual cortices in the alert cat. J Neurosci 2004;24:1627–1636. [PubMed: 14973243]

Salin PA, Bullier J. Corticocortical connections in the visual system: structure and function. Physiol Rev 1995;75:107–154. [PubMed: 7831395]

Scannell JW, Blakemore C, Young MP. Analysis of connectivity in the cat cerebral cortex. J Neurosci 1995;15:1463–1483. [PubMed: 7869111]

Schmitt WB, Arianpour R, Deacon RMJ, Seeburg PH, Sprengel R, Rawlins JNP, Bannermann DM. The role of hippocampal glutamate receptor-A-dependent synaptic plasticity in conditional learning: the importance of spatiotemporal discongruity. J Neurosci 2004;24:7277–7282. [PubMed: 15317854]

Schoups A, Vogels R, Qian N, Orban GA. Practising orientation identification improves orientation coding in V1 neurons. Nature 2001;412:549–553. [PubMed: 11484056]

Segraves MA, Rosenquist AC. The afferent and efferent callosal connections of retinotopically-defined areas in cat cortex. J Neurosci 1982a;2:1090–1107. [PubMed: 6180150]

Segraves MA, Rosenquist AC. The distribution of the cells of origin of callosal projections in cat visual cortex. J Neurosci 1982b;2:1079–1089. [PubMed: 6180149]

Sherk H. Coincidence of patchy inputs from the lateral geniculate complex and area 17 to the cat's Clare-Bishop area. J Comp Neurol 1986a;253:105–120. [PubMed: 2432097]

Sherk H. Location and connections of visual cortical areas in the cat's suprasylvian sulcus. J Comp Neurol 1986b;247:1–31. [PubMed: 2423562]

Sherk H, Mulligan KA. A reassessment of the lower visual field map in striate-recipient lateral suprasylvian cortex. Vis Neurosci 1993;10:131–158. [PubMed: 7678750]

Shi SH, Hayashi Y, Petralia RS, Zaman SH, Wenthold RJ, Svoboda K, Malinow R. Rapid spine delivery and redistribution of AMPA receptors after synaptic NMDA receptor activation. Science 1999;284:1811–1816. [PubMed: 10364548]

Shipp S, Grant S. Organization of reciprocal connections between area 17 and the lateral suprasylvian area of cat visual cortex. Vis Neurosci 1991;6:339–355. [PubMed: 1711892]

Song I, Huganir RL. Regulation of AMPA receptors during synaptic plasticity. Trends Neurosci 2002;25:578–588. [PubMed: 12392933]

Symonds LL, Rosenquist AC. Corticocortical connections among visual areas in the cat. J Comp Neurol 1984;229:1–38. [PubMed: 6490972]

Taub E, Uswatte G, Elbert T. New treatments in neurorehabilitation founded on basic research. Nat Rev Neurosci 2002;3:228–236. [PubMed: 11994754]

Tighilet B, Huntsman MM, Hashikawa T, Murray KD, Isackson PJ, Jones EG. Cell-specific expression of type II calcium/calmodulindependent protein kinase isoforms and glutamate receptors in normal and visually-deprived lateral geniculate nucleus of monkeys. J Comp Neurol 1998;390:278–296. [PubMed: 9453671]

Tsumoto T. Excitatory amino acid transmitters and their receptors in neural circuits of the cerebral cortex. Neurosci Res 1990;9:79–102. [PubMed: 1980528]

Tsumoto T, Hagihara K, Sato H, Hata Y. NMDA receptors in the visual cortex of young kittens are more effective than those of the adult. Nature 1987;327:513–514. [PubMed: 3035381]

Tusa RJ, Rosenquist AC, Palmer LA. Retinotopic organization of areas 18 and 19 in the cat. J Comp Neurol 1979;185:657–678. [PubMed: 447876]

Tusa, RJ.; Palmer, LA.; Rosenquist, AC. Multiple cortical visual areas. Visual field topography in the cat. In: Woolsey, CN., editor. Cortical sensory organisation. Clifton, NJ: Humana Press; 1981. p. 1-31.

Van Damme K, Massie A, Vandesande F, Arckens L. Distribution of the AMPA2 glutamate receptor subunit in adult cat visual cortex. Brain Res 2003;960:1–8. [PubMed: 12505651]

Vickers JC, Huntley GW, Edwards AM, Moran T, Rogers SW, Heinemann SF, Morrison JH. Quantitative localization of AMPA/kainate and kainate glutamate receptor subunit immunoreactivity in neurochemically identified subpopulations of neurons in prefrontal cortex of the macaque monkey. J Neurosci 1993;13:2982–2992. [PubMed: 7687283]

Vissavajjhala P, Janssen WG, Hu Y, Gazzaley AH, Moran T, Hof PR, Morrison JH. Synaptic distribution of the AMPA-GluR2 subunit and its colocalization with calcium-binding proteins in rat cerebral cortex: an immunohistochemical study using a GluR2-specific monoclonal antibody. Exp Neurol 1996;142:296–312. [PubMed: 8934561]

Wang C, Waleszczyk WJ, Burke W, Dreher B. Modulatory influence of feedback projections from area 21a on neuronal activities in striate cortex of the cat. Cereb Cortex 2000;10:1217–1232. [PubMed: 11073871]

Weibull W. A statistical distribution function of wide applicability. J Appl Mech 1951;18:292–297.

Wenthold RJ, Prybylowski K, Standley S, Sans N, Petralia RS. Trafficking of NMDA receptors. Annu Rev Pharmacol Toxicol 2003;43:335–358. [PubMed: 12540744]

Xerri C. Plasticity of primary somatosensory cortex parallelling sensorimotor skill recovery from stroke in adult monkeys. J Neurophysiol 1998;79:2119–2148. [PubMed: 9535973]

Xerri C, Benelhadj M, Harlay F. Deficits and recovery of body stabilization during acrobatic locomotion after focal lesion to the somatosensory cortex: a kinematic analysis combined with cortical mapping. Arch Ital Biol 2004;142:217–236. [PubMed: 15266656]

Yamasaki DS, Wurtz RH. Recovery of function after lesions in the superior temporal sulcus in the monkey. J Neurophysiol 1991;66:65–673.
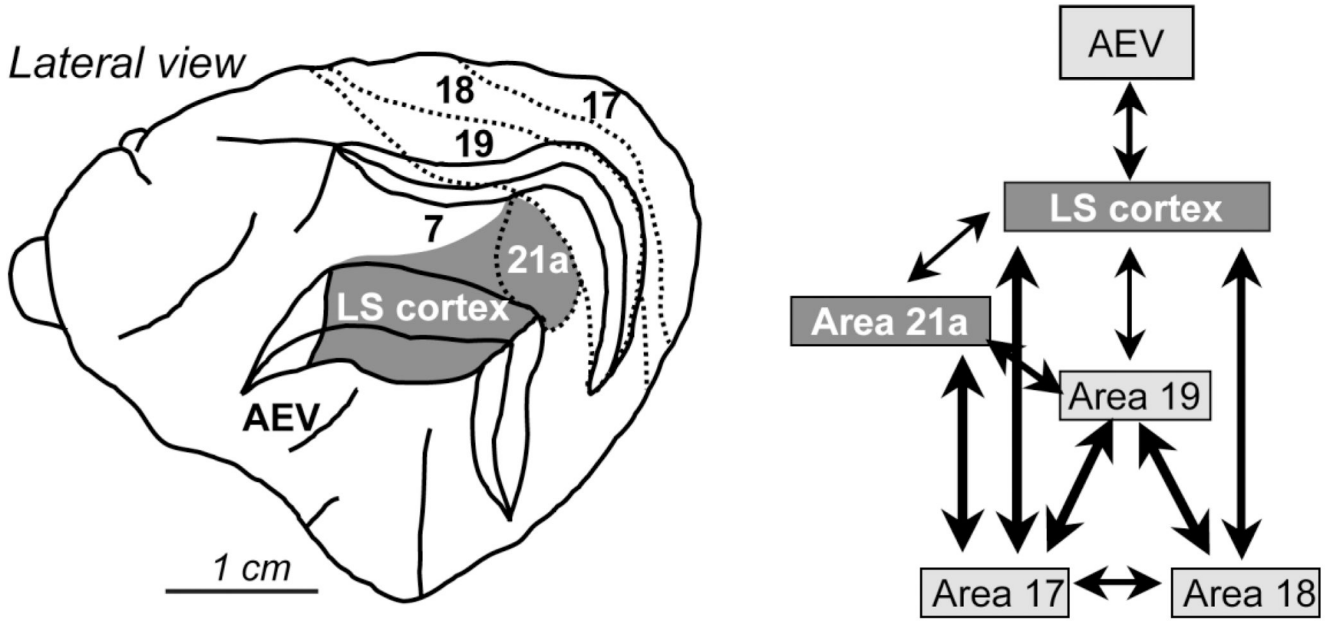
Fig. 1.
Visual cortical areas in the cat. Lateral view of the cat brain, illustrating the relative location of principal visual cortical areas. The adjacent schematic diagram is a simplified rendition of connectivity between these different visual cortical areas. It demonstrates the strong, direct interconnection between lower level visual areas (17, 18, and 19) and LS cortex. Dark gray shading indicates visual areas damaged in the present study. AEV, anterior ectosylvian visual area; LS, lateral suprasylvian.
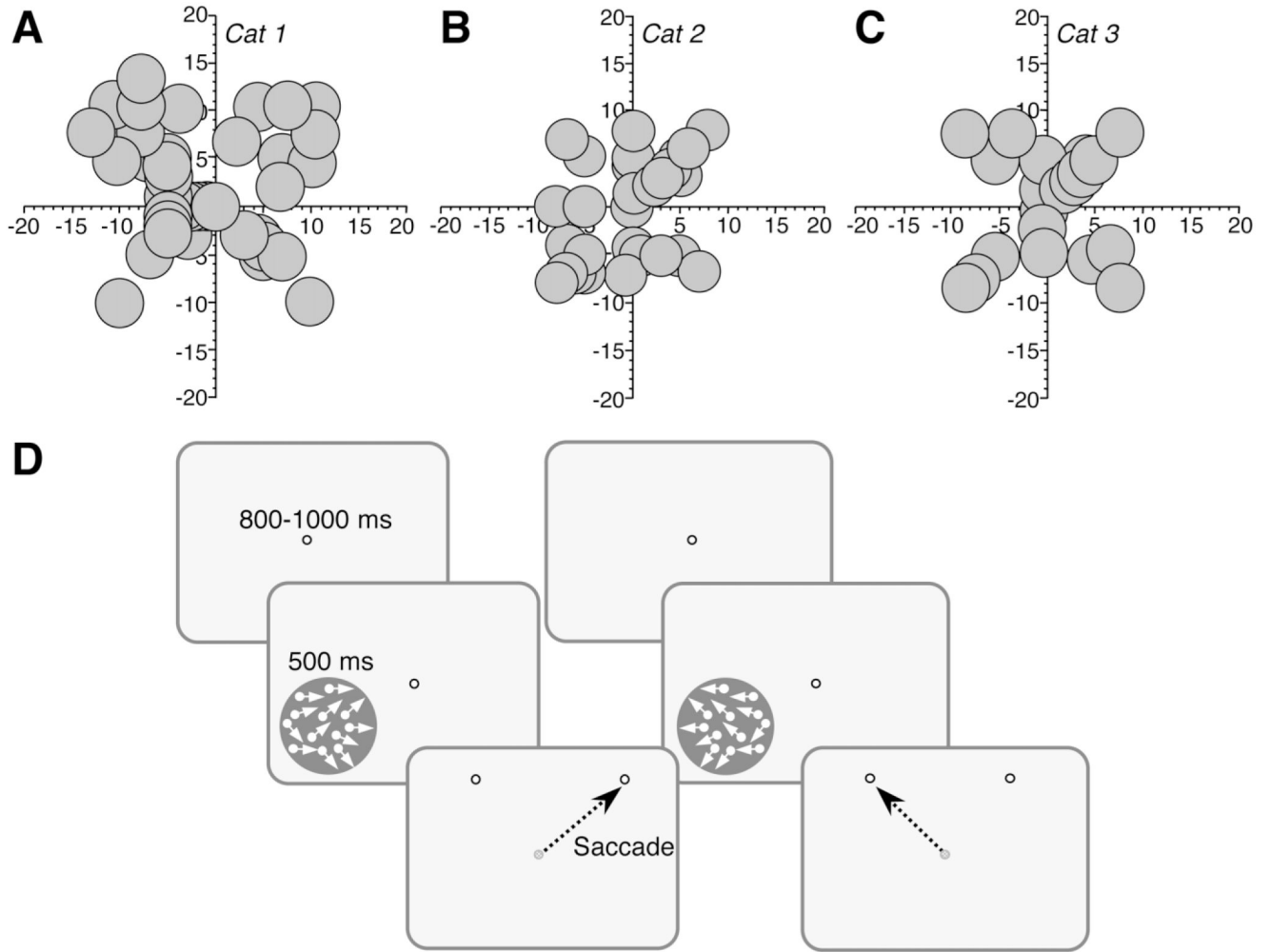
Fig. 2.
Behavioral training paradigm. **A–C:** Maps of visual field space illustrating the location, size, and shape of visual stimuli used during initial, prelesion training of direction discrimination in Cats 1, 2, and 3. Axes are labeled in degrees of visual angle. Note the relative symmetry of trained locations across the vertical meridian. **D:** Direction discrimination task used to train and test cats before and after LS lesions. First, a fixation spot appeared on the computer monitor, and the animals had to fixate it for 800–1,000 ms in order for a random dot stimulus to appear. The stimulus drifted either leftward or rightward for 500 ms, during which the cats were required to maintain fixation on the central target. After 500 ms, the stimulus and fixation target disappeared and were replaced by two "response" spots. The cats were required to saccade to the rightmost spot on the monitor if the global direction of motion of the stimulus had been to the right, and to the leftmost spot if the global direction of motion had been to the left.
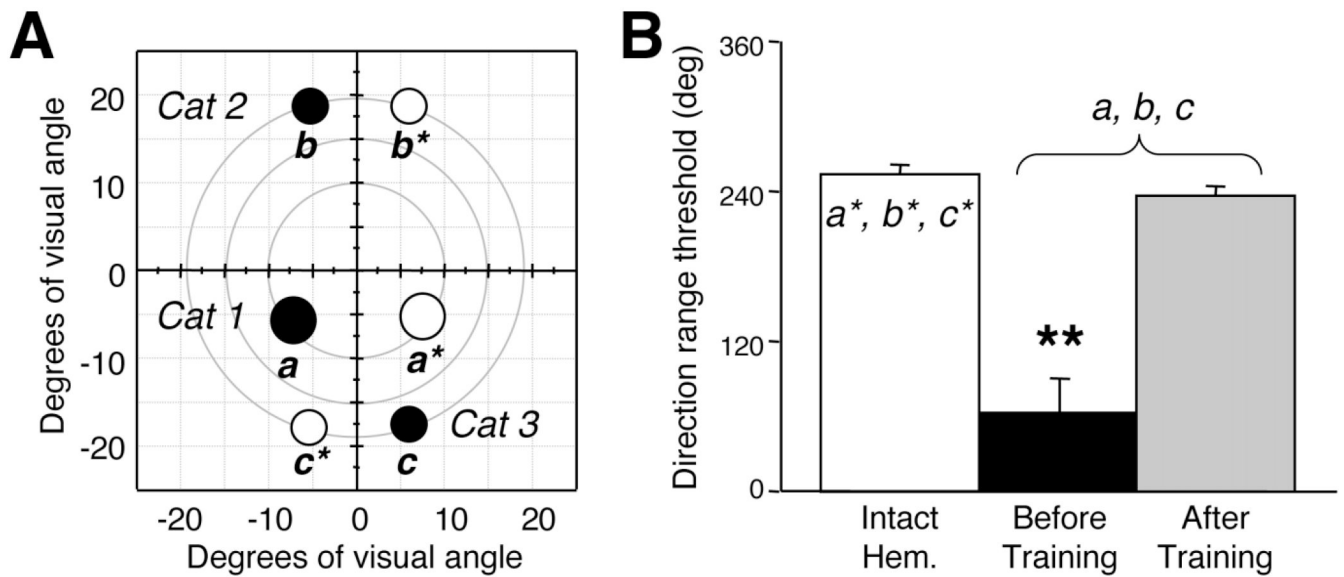
Fig. 3.
Location of visual retraining after LS lesions in Cats 1, 2, and 3. **A:** Visual field map illustrating visual field locations chosen for retraining (black circles labeled a, b, and c) in the impaired hemifields of Cats 1, 2, and 3. Performance was also mapped at corresponding, control locations in the intact hemifields of Cats 1, 2, and 3 (white circles labeled a*, b*, and c*). **B:** Histogram plotting mean direction range thresholds at control and retrained locations (shown in A), averaged among Cats 1, 2, and 3. The white bar indicates thresholds at control locations (a*, b*, and c* in A) in the intact hemifields, where cats can tolerate a large range of dot directions and still correctly perceive the global direction of motion of the random dot stimulus. Black and gray bars show performance at contralesional locations a, b, and c (shown in A) before (black) or after (gray) direction discrimination training by using random dot stimuli in which the range of dot directions was varied. Note the significantly abnormal performance before the onset of training and the recovery to normal direction range thresholds after training. Error bars = standard deviations. **, $P < 0.05$, by two-tailed Student's t-test.
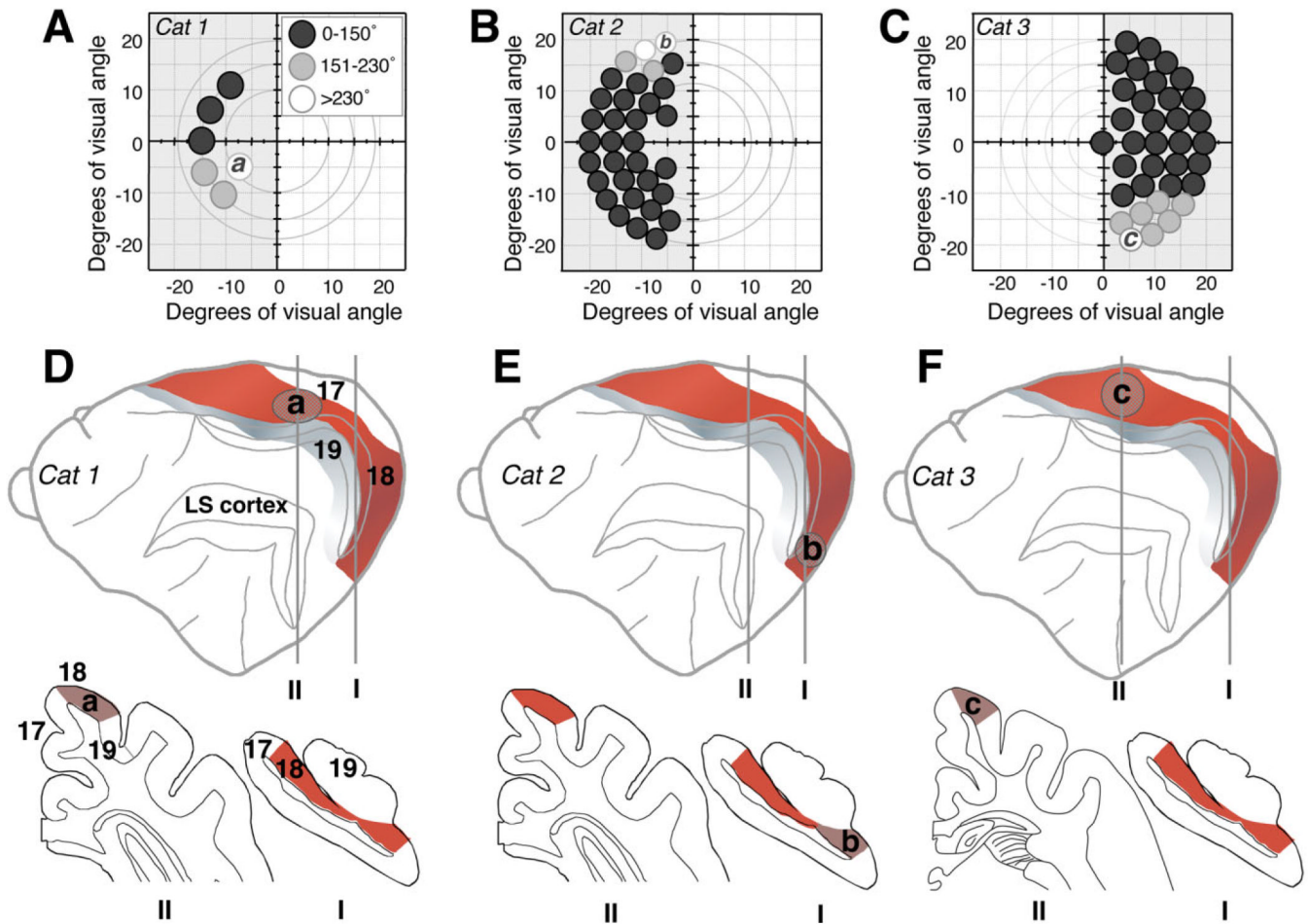
Fig. 4.
Retinotopy of training-induced visual recovery in Cats 1, 2, and 3. **A–C:** Maps of the visual field in Cats 1, 2, and 3 illustrating, via the indicated gray scale, the magnitude of training-induced improvements in direction range thresholds (relative to immediate postlesion performance) at locations "a", "b," and "c" within the contralesional, impaired hemifields, as well as at several adjacent locations. Circles (drawn to scale) represent the size and position of random dot stimuli used to measure direction range thresholds at each of the locations tested. White circles denote the largest improvements attained, which averaged above 230° of direction range and resulted in recovery to normal levels of performance relative to equivalent locations in the intact hemifield. Light gray circles indicate moderate improvements to less than normal levels of performance. Dark gray circles denote little to no improvement. **D–F:** Schematic diagrams indicating the approximate locations of regions within area 18 that corresponded retinotopically to retrained locations "a," "b," and "c" in Cats 1 (D), 2 (E), and 3 (F), respectively. The lateral views of the cat brain are displayed in an "open sulcus" configuration, and illustrate the location of cortical area 18 (red shading) relative to areas 17 (white), 19 (gray), and LS cortex (damaged in all three cats). Coronal sections (traced by using the NeuroLucida software) from locations I (~7 mm posterior to the interaural line) and II (~1 mm anterior to the interaural line for Cat 2 and ~8 mm anterior to the interaural line for Cat 3) illustrate the different retinotropic regions of area 18 selected for analysis. According to the electrophysiological maps of Tusa and colleagues (1979, 1981), the area 18 representation of location "a" in the mid-lower field is more anterior and dorsal than the brain location of far

upper field region "b," but it is more posterior than the brain location where the far lower field location "c" is represented.
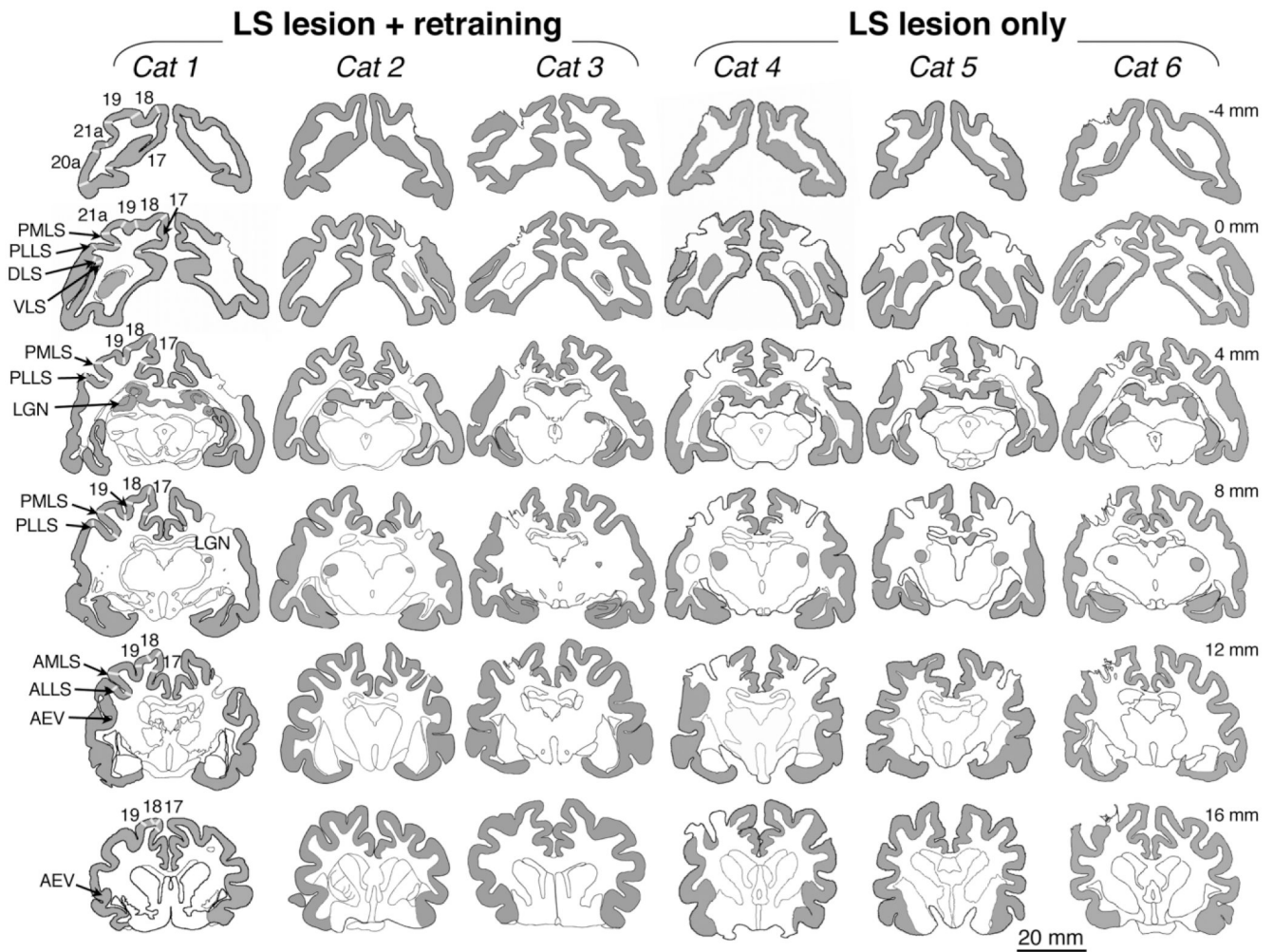
Fig. 5.
Lesion reconstructions. Brain sections stained for cytochrome oxidase (gray shading in cortex and lateral geniculate nucleus) were reconstructed by using the NeuroLucida software. Visual cortical areas of interest are labeled in the left hemisphere of Cat 1, with white lines separating the different areas. LGN, lateral geniculate nucleus; AMLS, anteromedial lateral suprasylvian visual area; ALLS, anterolateral lateral suprasylvian visual area; PMLS, posteromedial lateral suprasylvian visual area; PLLS, posterolateral lateral suprasylvian visual area; DLS, dorsal lateral suprasylvian visual area; VLS, ventral lateral suprasylvian visual area; AEV, anterior ectosylvian visual area. Approximate anteroposterior location of the sections in each row is indicated in mm relative to the interaural line. Negative values are located posterior, and positive values are anterior to the interaural line. Note the areas of missing gray matter around the lateral suprasylvian sulcus in the right hemisphere of Cats 1, 2, 4 and 5 and the left hemisphere of Cats 3, 4, 5, and 6. Areas PMLS and PLLS were completely destroyed in all cats, with no islands of spared tissue. In addition, there was extensive, often complete damage to areas VLS, DLS, 21a, AMLS, and ALLS. A small part of area 19 was also damaged in Cats 3–6, but areas 17 and 18 and AEV were completely intact in all cats.
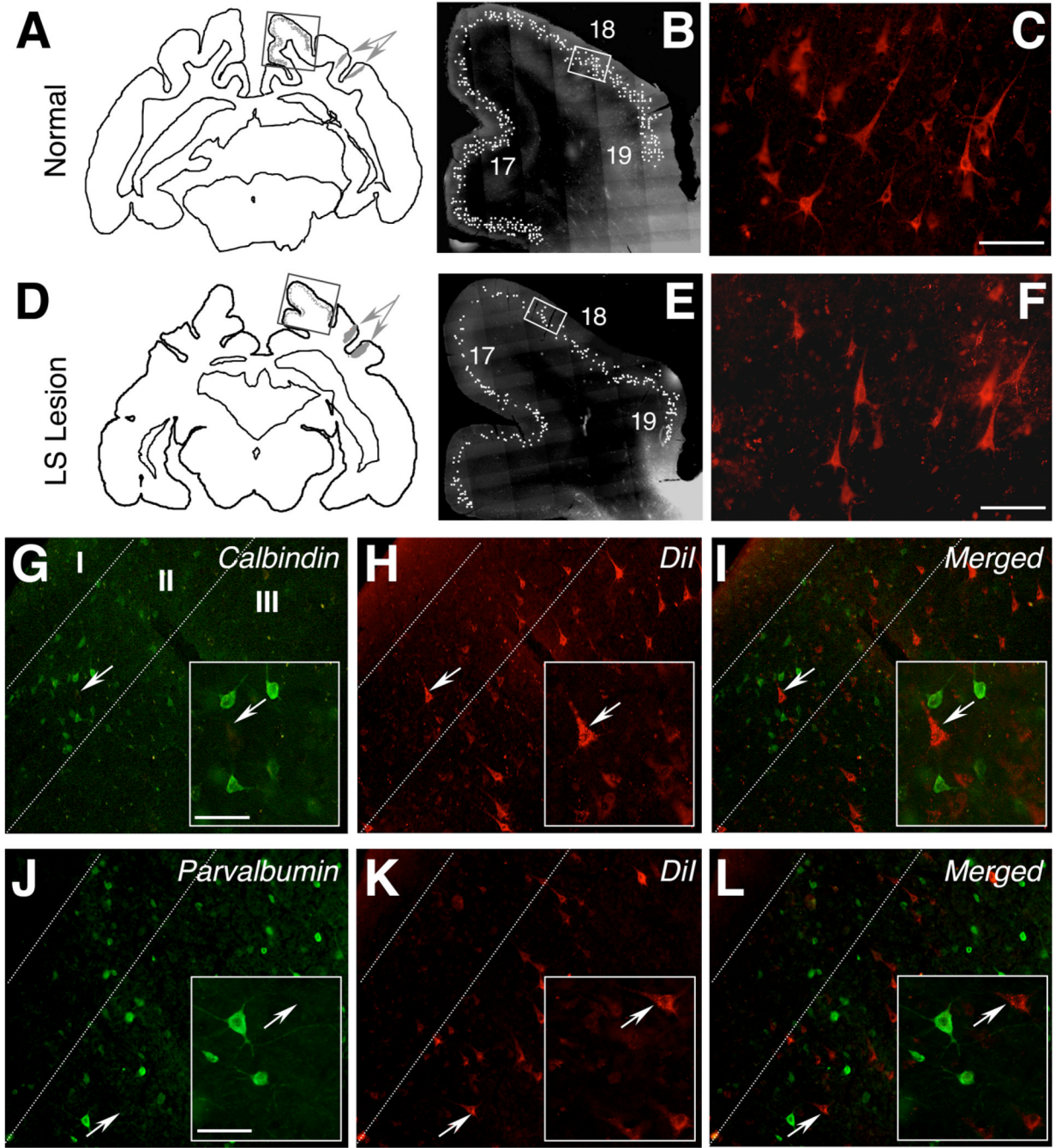
Fig. 6.
Neuronal labeling in supragranular layers of area 18. **A:** Distribution of LS-projecting cells in a normal cat (Cat 7) illustrated in a NeuroLucida tracing of a coronal brain section. The section shows two DiI injection sites, one into each bank of the LS sulcus (gray arrows), and the distribution of retrogradely labeled cells (gray dots) in areas 17, 18, and 19. **B:** Photomontage of the rectangular region outlined in A, illustrating the supragranular distribution of labeled cells, each marked with a white dot. **C:** High-power photomicrograph of DiI-labeled, LS-projecting cells in area 18, highlighting the pyramidal morphology of these cells. **D:** NeuroLucida tracing of a coronal brain section from Cat 4, who had received injections of DiI into LS cortex 2 weeks prior to damaging LS cortex. **E:** Photomontage of the rectangular region

outlined in D, illustrating the supragranular distribution of labeled cells, each marked with a white dot. **F:** High-power photomicrograph of DiI-labeled, LS-projecting cells in area 18 of Cat 4. Note the significant number of DiI-labeled cells, which survive for several months after the lesion. **G:** Area 18 of a normal cat showing the distribution of neurons expressing calbindin (green) in supragranular layers (II and III). Cortical layers I, II, and III are separated by dashed white lines. The white arrow indicates a calbindin-negative pyramidal cell, which is magnified in the inset. **H:** Same field as in G, viewed under rhodamine fluorescence, to illustrate DiI-labeled cells. Note the arrowed pyramidal cell, whose location is marked in G–I. **I:** Merged images from G and H, demonstrating a complete lack of colocalization between calbindin and DiI. **J:** Area 18 of a normal cat showing the distribution of neurons expressing parvalbumin (green) in supragranular layers. The white arrow indicates a parvalbumin-negative pyramidal cell, which is magnified in the inset. **K:** Same field as in J, viewed under rhodamine fluorescence, to show DiI-labeled cells. Note the arrowed pyramidal cell, originally shown in J. **I:** Merged images from J and K, demonstrating a complete lack of colocalization between parvalbumin and DiI. Labeling conventions as in G–I. A magenta-green version of this figure can be found online for color-blind readers. Scale bar = 100 µm in C (applies to B,C), F (applies to E,F), and insets to G,J (applies to insets in G–L.
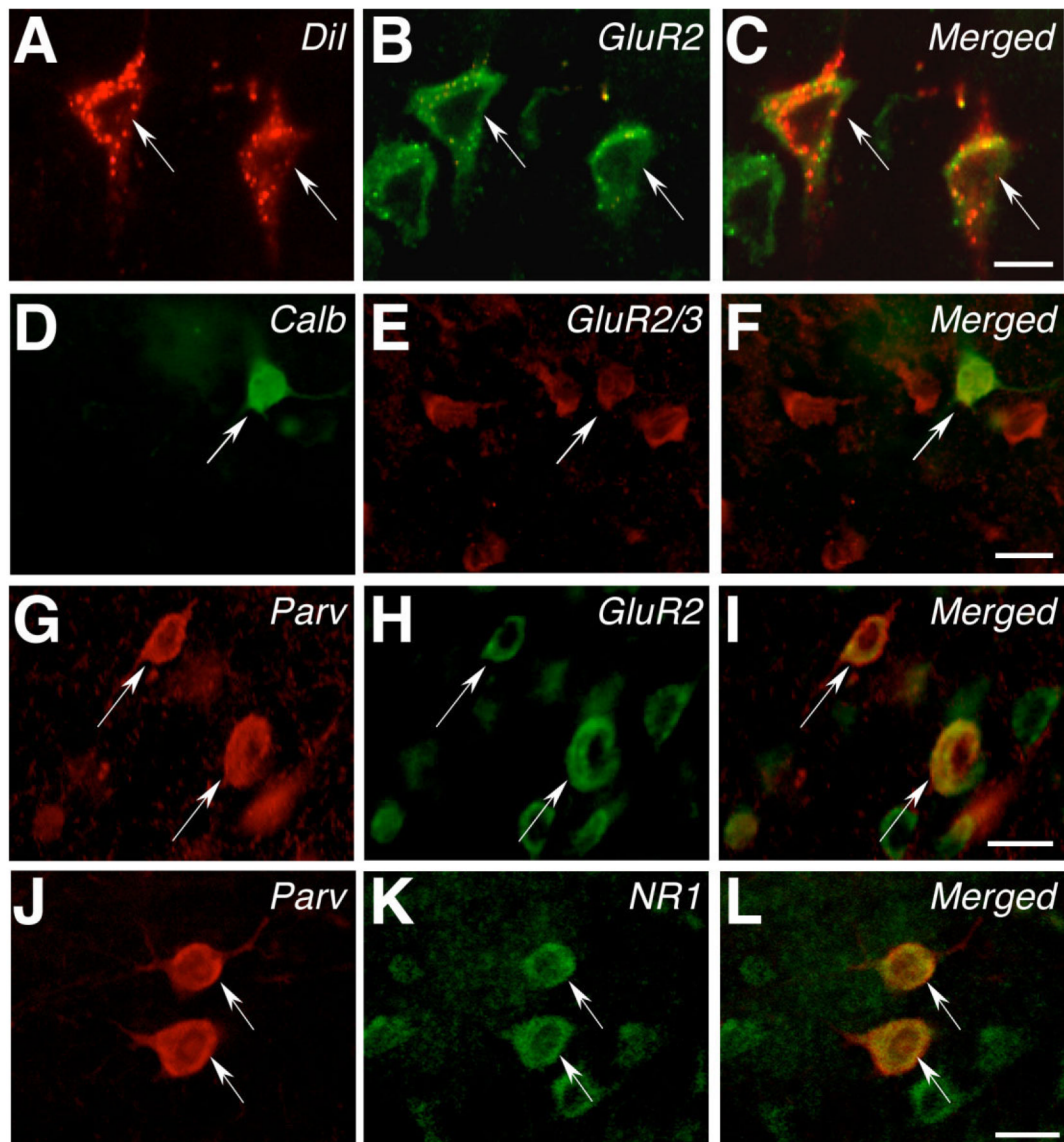
Fig. 7.
AMPAR and NMDAR subunit expression in supragranular layers of area 18. **A:** High-power photomicrograph illustrating two DiI-positive cells in supragranular layers of area 18 (arrowed). **B:** Same field of view as in A, showing staining for the GluR2 subunit of the AMPAR. **C:** Merged image of A and B, showing that the two arrowed DiI-positive cells express the GluR2 subunit of the AMPAR. **D:** High-power photomicrograph illustrating a calbindin-positive cell in supragranular layers of area 18 (arrowed). **E:** Same field of view as in D, showing staining for GluR2/3. **F:** Merged image of D and E, showing that the arrowed calbindin-positive cell expresses GluR2/3. **G:** High-power photomicrograph illustrating two parvalbumin-positive cells in supragranular layers of area 18 (arrowed). **H:** Same field of view as in G, showing staining for the GluR2 subunit of the AMPAR. **I:** Merged image of G and H, showing that the two arrowed cells express the GluR2 subunit of the AMPAR. **J:** High-power photomicrograph illustrating two parvalbumin-positive cells in supragranular layers of area 18 (arrowed). **K:** Same field of view as in J, showing staining for the NR1 subunit of the NMDAR. **L:** Merged image of J and K, showing that the two arrowed cells express NR1. A magenta-

green version of this figure can be found online for colorblind readers. Scale bar = 20 µm in C (applies to A–C), F (applies to D–F), I (applies to G–I), and L (applies to J–L).

TABLE 1

Percentage of Supragranular Neurons in Area 18 Expressing Different Glutamate Receptor Subunits

Cell type	GluR1	GluR2	GluR2/3	GluR4	NMDAR1
LS-projecting cells					
Control					
No lesion	97 ± 1.7	95 ± 1.0	96 ± 1.0	98 ± 0.9	98 ± 2.3
LS lesion	**81 ± 4.1**	95 ± 1.5	94 ± 0.5	93 ± 0.7	95 ± 1.7
Trained					
Retrained region	98 ± 0.9	96 ± 0.2	96 ± 0.5	99 ± 0.4	98 ± 1.3
Untrained region	**85 ± 3.4**	94 ± 0.2	95 ± 1.0	93 ± 2.0	—
Calbindin-positive cells					
Control					
No lesion	97 ± 1.6	95 ± 1.7	91 ± 0.3	97 ± 0.8	95 ± 1.0
LS lesion	**84 ± 4.6**	**73 ± 3.5**	79 ± 2.6	80 ± 3.7	94 ± 1.2
Trained					
Retrained region	96 ± 1.3	**96 ± 0.9**	88 ± 0.6	94 ± 1.3	97 ± 0.6
Untrained region	**88 ± 0.8**	**80 ± 3.7**	**79 ± 1.8**	**90 ± 0.7**	—
Intact hemisphere	**86 ± 1.4**	**80 ± 3.9**	**80 ± 1.1**	**91 ± 1.9**	—
Parvalbumin-positive cells					
Control					
No lesion	99.5 ± 0.4	95 ± 2.3	96 ± 1.5	98 ± 0.7	94 ± 0.6
LS lesion	95 ± 1.8	**79 ± 3.7**	**66 ± 4.2**	97 ± 1.5	92 ± 0.5
Trained					
Retrained region	98 ± 0.7	96 ± 1.8	95 ± 1.7	98 ± 0.5	89 ± 2.8
Untrained region	98 ± 0.2	95 ± 2.0	96 ± 0.5	99 ± 0.4	89 ± 4
Intact hemisphere	96 ± 0.9	**88 ± 0.6**	**82 ± 3.4**	98 ± 0.6	—

[1] Values are means ± SEM "Control" represents data from control cats that never underwent visual training. "Trained" represents data from cats that underwent visual retraining to recovery after a unilateral lesion of LS cortex. Bold numbers indicate statistical significance at the $P < 0.05$ level (two-tailed Student's t-text) relative to the "No lesion" control condition. Abbreviations: GluR, glutamate receptor; LS, lateral suprasylvian (sulcus); NMDAR, N-methyl-D-aspartate receptor.